



**INSTITUTO POTOSINO DE INVESTIGACIÓN
CIENTÍFICA Y TECNOLÓGICA, A.C.**

POSGRADO EN NANOCIENCIAS Y MATERIALES

**“Complex network characteristics in the mycelium
of *Trichoderma atroviride*”**

Tesis que presenta

Edgar Martínez Galicia

Para obtener el grado de

Maestro(a) en Nanociencias y Materiales

Director de la Tesis:

Dr. Braulio Gutiérrez Medina

San Luis Potosí, S.L.P., mes de año



Constancia de aprobación de la tesis

La tesis “**Complex networks characteristics in filamentous networks of *Trichoderma atroviride*.**” presentada para obtener el Grado de Maestro(a) en Nanociencias y Materiales fue elaborada por **Edgar Martínez Galicia** y aprobada el **5 de noviembre del 2021** por los suscritos, designados por el Colegio de Profesores de la División de Materiales Avanzados del Instituto Potosino de Investigación Científica y Tecnológica, A.C.

Dr. Braulio Gutiérrez Medina

Director de la tesis

Dr. Haret-Codratian Rosu Barbus

Miembro del Comité Tutorial

Dr. José Luis Sánchez Salas

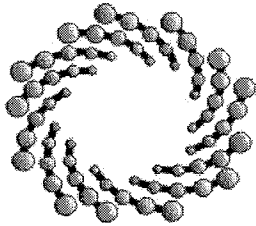
Miembro del Comité Tutorial



Créditos Institucionales

Esta tesis fue elaborada en el Laboratorio de Nanomateriales I de la División de Materiales Avanzados del Instituto Potosino de Investigación Científica y Tecnológica, A.C., bajo la dirección del Dr. Braulio Gutiérrez Medina.

Durante la realización del trabajo el autor recibió una beca académica del Consejo Nacional de Ciencia y Tecnología (1006980) y del Instituto Potosino de Investigación Científica y Tecnológica, A. C.



IPICYT

Instituto Potosino de Investigación Científica y Tecnológica, A.C.

Acta de Examen de Grado

El Secretario Académico del Instituto Potosino de Investigación Científica y Tecnológica, A.C., certifica que en el Acta 075 del Libro Primero de Actas de Exámenes de Grado del Programa de Maestría en Nanociencias y Materiales está asentado lo siguiente:

En la ciudad de San Luis Potosí a los 16 días del mes de noviembre del año 2021, se reunió a las 16:00 horas en las instalaciones del Instituto Potosino de Investigación Científica y Tecnológica, A.C., el Jurado integrado por:

Dr. Haret-Codratian Rosu Barbus
Dr. Braulio Gutiérrez Medina
Dr. José Luis Sánchez Salas

Presidente
Secretario
Sinodal externo

IPICYT
IPICYT
UDLAP

a fin de efectuar el examen, que para obtener el Grado de:

MAESTRO EN NANOCIENCIAS Y MATERIALES

sustentó el C.

Edgar Martínez Galicia

sobre la Tesis intitulada:

Complex network characteristics in the mycelium of Trichoderma atroviride

que se desarrolló bajo la dirección de

Dr. Braulio Gutiérrez Medina

El Jurado, después de deliberar, determinó

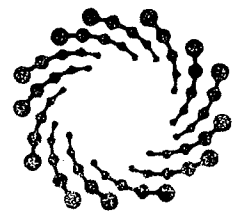
APROBARLO

Dándose por terminado el acto a las 17:45 horas, procediendo a la firma del Acta los integrantes del Jurado. Dando fe el Secretario Académico del Instituto.

A petición del interesado y para los fines que al mismo convengan, se extiende el presente documento en la ciudad de San Luis Potosí, S.L.P., México, a los 16 días del mes de noviembre de 2021.

Mtra. Ivonne Lizette Cuevas Vález
Jefa del Departamento del Posgrado

Dr. Marcial Bonilla Marín
Secretario Académico



IPICYT
SECRETARÍA ACADÉMICA
INSTITUTO POTOSINO DE
INVESTIGACIÓN CIENTÍFICA
Y TECNOLÓGICA, A.C.

Dedicatoria

La culminación de este documento representa no solo un logro personal sino un invaluable apoyo de familiares, pareja y amigos.

Esta tesis está dedicada para todos ustedes.

Agradecimientos

Al **IPICYT** por la formación académica, sus excelentes profesores y las instalaciones.

Al **Consejo Nacional de Ciencia y Tecnología** por la beca otorgada para alcanzar este logro personal y representar el potencial de la ciencia mexicana.

Al **Dr. Braulio Gutiérrez Medina** por su constante guía, enseñanza y paciencia a lo largo de la realización de este proyecto.

Al **Comité tutorial** por su apoyo y asesoramiento fundamental en la realización de este proyecto.

Resumen

Las redes complejas se han estudiado desde el siglo pasado con gran interés debido a su creciente presencia en el mundo moderno, gracias a redes sociales, el internet, redes de tránsito aéreo, marítimo, entre otras. El estudio de estos sistemas ha cambiado con el paso del tiempo, adoptando métodos matemáticos para su comprensión debido al incremento de elementos contenidos en estas. Una red compleja está formada por nodos y aristas, los nodos son definidos como puntos en un espacio y están unidos o conectados por aristas, las cuales son líneas. Ambos elementos pueden tener distintas características repercutiendo en la complejidad de la red; por ejemplo, un nodo puede tener una o más conexiones, lo cual aumenta su importancia en la red. Por otro lado, una arista puede ser discreta o directa, entre más aristas discretas haya, más compleja se vuelve la red.

Las redes mencionadas anteriormente no son las únicas que se estudian, también hay una rama que estudia redes biológicas, tales como, las redes neuronales en el cerebro, rutas metabólicas, hongos filamentosos, entre otros. En este trabajo nos enfocaremos en la extracción de parámetros asociadas a una de red compleja de micelios en hongos filamentosos, los cuales tiene la característica de que sus células se presentan de forma alargada formando ramas llamadas hifas y entre ellas se conectan por anastomosis. Está red tiene el paralelismo con una red compleja debido a que las hifas son las aristas y los cruces donde se conectan las hifas son los nodos, de esta manera se crea una red. El hongo filamentoso que se estudió en este trabajo es *Trichoderma atroviride*, que habita de manera natural sobre la madera muerta en los suelos de los bosques por lo que se considera un saprófito.

El análisis se llevó a cabo siguiendo una serie de pasos, en donde el primer paso fue incubar al hongo, con mejores condiciones para que su desarrollo sea el más conveniente para cumplir el objetivo del proyecto. El segundo paso consistió en fotografiar al hongo usando microscopía óptica de campo claro en distintos tiempos, para poder analizar el cambio de las propiedades de red en función del tiempo. Como tercera parte, se registraron los parámetros de red compleja, tales como el número de nodos, el grado de los nodos y las longitudes de las aristas, que

posteriormente se analizaron mediante un software especializado. Como última parte, los resultados obtenidos se propone que se analicen otros parámetros como el grado promedio de los nodos, longitud total y longitud promedio.

Palabras clave: redes complejas, nodos, aristas, hongos filamentosos, hifas, microscopía óptica, grados, longitudes.

Abstract

Complex networks have been studied since the last century with great interest due to their growing presence in the modern world, thanks to social networks, the internet, air traffic networks, maritime networks, among others. The study of these systems has changed over time, adopting mathematical methods for their understanding due to the increase of elements contained in them. A complex network is formed by nodes and edges, nodes are defined as points in a space and are joined or connected by edges, which are lines. Both elements can have different characteristics that affect the complexity of the network; for example, a node can have one or more connections, which increases its importance in the network. On the other hand, an edge can be discrete or direct; the more discrete edges there are, the more complex the network becomes.

The networks mentioned above are not the only ones studied, there is also a branch that studies biological networks, such as neural networks in the brain, metabolic pathways, filamentous fungi, among others. In this work we focus on the extraction of parameters associated with a complex network of mycelia in filamentous fungi, which have the characteristic that their cells are presented in an elongated form forming branches called hyphae and between them are connected by anastomoses. This network parallels a complex network because the hyphae are the edges and the junctions where the hyphae connect are the nodes, thus creating a network. The filamentous fungus studied in this work is *Trichoderma atroviride*, which naturally inhabits dead wood in forest soils and is therefore considered a saprophyte.

The analysis was carried out following a series of steps, where the first step was to incubate the fungus, with better conditions for its development to fulfil the objective of the project. The second step consisted of photographing the fungus using brightfield optical microscopy at different times, to analyse the change of the network properties as a function of time. As a third part, complex network parameters such as the number of nodes, node degree and edge lengths were recorded and analysed using specialized software. As a last part, the results obtained are proposed to

analyse other parameters such as average node degree, total length, and average length.

Keywords: complex networks, nodes, edges, filamentous fungi, hyphae, optical microscopy, degrees, lengths.

TABLE OF CONTENTS

CONSTANCIA DE APROBACIÓN DE LA TESIS	II
CRÉDITOS INSTITUCIONALES	III
ACTA DE EXAMEN.	IV
DEDICATORIA	V
AGRADECIMIENTOS	VI
RESUMEN	VII
ABSTRACT	IX
I. INTRODUCTION	13
Networks	16
Properties of Networks	17
Degree	17
Geodesic path and diameter	19
Clustering or Transitivity (T)	19
Small-world property	20
Filamentous fungi network	20
Filamentous fungi growth	21
Hyphae	22
Model system: <i>Trichoderma atroviride</i>	24
G – Hyphal Growth Unit	25
Our work	26
Hypothesis	27
General goals	27
Specific goals	27
II. RESEARCH METHODOLOGY	28
Mycelium growth	29
Spore´s germination	30

Brightfield optical microscopy	30
Image acquisition and processing	31
Digital processing	31
Pre-processing steps	32
Mosaic assembly	39
Network extraction	40
NEFI stages	42
Statistical Analysis	43
G – Hyphal growth unit	45
III. RESULTS	46
Mycelium growth	47
Spore’s germination	50
Image acquisition and digital processing	51
Mosaic assembly	52
Network Extraction	55
Statistical analysis	60
G – Hyphal growth unit	65
Conclusions and Perspectives	68
Annex	69
IV. BIBLIOGRAPHY	85

I. Introduction

Complex networks are around us in different ways, some of them are not tangible like internet, air traffic, us by conforming a social media, but another is tangible like subway lines, biological systems like neurons, mycelia, among others. (Watts, D. J., & Strogatz, 1998). The study of networks started with a branch of discrete mathematics called graph theory developed by Leonard Euler in 1736 solving the Königsberg bridge problem. (Amaral & Ottino, 2004). In 1920's, the analysis of social interactions has started, focusing on the relationships among social entities. (Boccaletti et al., 2006). In the 1950's the largest network was described as random graphs, because it is the simplest and most straightforward concept in graph theory. (Albert & Barabási, 2002).

In recent years, networks have an irregular structure and dynamic evolution, increasing their complexity. (Albert & Barabási, 2002). Therefore, to characterize new complex networks, new concepts and measures were proposed, such as small world, clustering and degree distribution, which use common principles and statistical properties to define the networks (Albert & Barabási, 2002; Boccaletti et al., 2006).

A network is defined as the collection of dots connected each other by lines.

Each dot is called vertex (graph theory), a node (computer science) a site (physics) or an actor (sociology) and each line is called edge (graph theory), bond (physics) or link (computer science) or a tie (sociology). (M. E. J. Newman, 2003).

There are many worthy aspects of study, like the nature of individual parts, connections or interactions and patterns of connections. The network itself may be represented as a pattern, having individual parts as nodes and connections as edges. Through the years, a set of mathematical, computational, and statistical tools have been developed to analyse, modelling, and understanding networks from a simple network representation and performing corresponding calculations useful information can be provided. In other words, networks are a means for representing patterns between the parts of a system. One of the main reasons of studying networks is because of data transport (M. Newman, 2013).

With the passing of the years, many networks have been discovered in biological systems, such as the neural networks. The study of neural networks has been treated by different methods, some of them are mathematical and stochastic methods, resulting the Network Science (Baronchelli et al., 2013). This science applies graph theory in neuroimaging to describe the active relationship between neural networks and their change, great importance in matters of age, health and disease (Ash & Rapp, 2014).

Another biological network is the mycelial fungi, which form an interconnected network with a high response to local environmental conditions. The difference with respect to other biological networks, such as transport system of plants or animal vascular system is that the network is the fungi organism itself, not just part of it. Mycelium is formed by growth of apical extension in hyphae with branches apically or sub-apically. (Horio, 2007).

The structure of mycelium fungi networks is described by Ascomycete's mycelium cells, which have septa with pores among cells to allow cytoplasm continuity and organelle movement through the structure. Some fungi combine tip growth and branching to explore and sense their environment using a range of efficient species-specific space searching adapting algorithms. Anastomoses occurs

behind the colony to form an interconnected microscopic mycelial network (Heaton et al., 2012).

In some basidiomycetes, the network architecture develops a specialised high-conductivity organ, called cords or rhizomorphs. Mature cords internal anatomy varies into basidiomycetes but share the same internal structure. They have a central inner medulla containing rigid hollow vessels hyphae with diameters from 10 to 15 μm and septal pores for translocation (Cairney, 2005). Cords are covered with an external cortex for the exchange of water and solutes. In addition, some parts of mycelium expand and mature, other regions retreat and bring autophagy process being critical to recycle material to support new growth. This process could be observed when new resources are encountered while mycelium is expanding (Boddy, 1999). Furthermore, mycelial fungi form the most extensive biological networks, known as Wood Wide Web (Smith, M. L., Bruhn, J. N., & Anderson, 1992).

The concept of fractal dimension is employed as a useful tool to study networks structure as a metric. Also, tools from graph theory bring more detailed characterisation of networks structure and dynamics and even allow exploration of underlying mechanism to improve networks. Due to the large number of interconnections these approaches needs all branching points and linking cords to be digitised, requiring semi-automated network extraction techniques (Heaton et al., 2012).

These methods require specific culture conditions from natural environment, which are crucial to explore the natural behavioural capability and the full range of ecological response of these organisms (Boddy, 1999). Apart from this, cords are multi-hyphal aggregates with variation in diameter from micrometres (μm) to millimetres (mm) in a single colony. Thus, it should be segmented from the background of compressed soil. Therefore, architecture network delineation has been only manually analysed (Bebber et al., 2007).

Networks

As was stated before, networks have vertices connected by edges in different ways, so that there could be more than one type of vertices and edges, with a variety of properties associated with them. If we consider the people of a community as a social network, vertices may represent men or women, locations, ages, incomes or any other characteristic, meanwhile, edges may represent friendship, animosity or professional acquaintance or geological proximity. In this way, vertices and edges could represent several things with different properties and meanings. They can be directed or undirected. When edges connected more than two vertices, they are called hyperedges, an example could be the family ties. Then we have bipartite graphs, which are graphs with two different types of vertices and edges only running between unlike types. In Figure 1 we can see the different types of networks. (M. E. J. Newman, 2003).

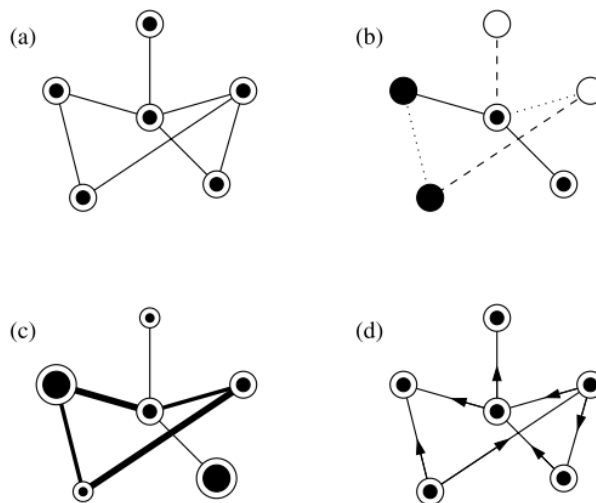


Figure 1. Different types of networks. a) undirected network with only a single type of vertices and edges. b) Network with several discrete vertices and edges. c) a network with different types of vertices and edges. d) a directed network, in which each edge has a direction

Complex networks have vertices with a higher hierarchy, related with the degree, which is the number of edges connected to a vertex. Also, this connection

is usually named node. If we want to know about the way between two nodes, there concept of geodesic path, which describe the shortest path through the network from one node to another, it could be more than one geodesic path for the same nodes. Furthermore, geodesic path could bring more information about the network, like the diameter, which is the longest geodesic path between two nodes. (M. E. J. Newman, 2003)

Properties of Networks

Complex networks have a wide diversity of measurable characteristics like geodesic path, diameter, degree distributions, clustering, small-world, and scale free properties, among others. But first, it is necessary to determine if the network is direct or indirect, this concept is related with the edges, when edges only have one direction, they are direct, therefore the network is directed if all of them are directed. Otherwise, undirected edges are when they run in both directions. If all of them meet this condition the network is undirected. (M. E. J. Newman, 2003). Some examples of directed networks are World Wide Web, e-mails and metabolic route (*Escherichia coli*), while undirected ones are protein interactions, peer-to-peer interactions and company directors. (Boccaletti et al., 2006; M. E. J. Newman, 2003). Once this characteristic is established, we could select the correct considerations to calculate other parameters and properties.

Degree

It is defined as the number of edges connected to a node. If edges are directed, then has both an in-degree and an out-degree for each node, which are the numbers of incoming and outgoing edges respectively. Otherwise, if edges are undirected only has a single number of degree. (Boccaletti et al., 2006)

Degree distribution ($\rho(k)$) is the probability that a node chosen randomly has

degree k . For example, undirected probability p is distributed according to a binomial distribution or in a Poisson distribution in the limit of large n . This distribution may be represented by a plot of cumulative distribution function, because an histogram with all nodes degree will have a left skew. (M. E. J. Newman, 2003)

$$P_k = \sum_{k'=k}^{\infty} p_{k'} \quad (1)$$

Where p_k is the probability that a vertex chosen randomly has degree k , P_k is the probability that a degree is higher or equal to k . This plot has the advantage that all data are represented, meanwhile, the conventional histogram by binning, any differences between values of data points that fall in the same bin are lost. (M. E. J. Newman, 2003). However, the plot P_k has a bias towards small values, so it is recommendable to make a binning histogram.

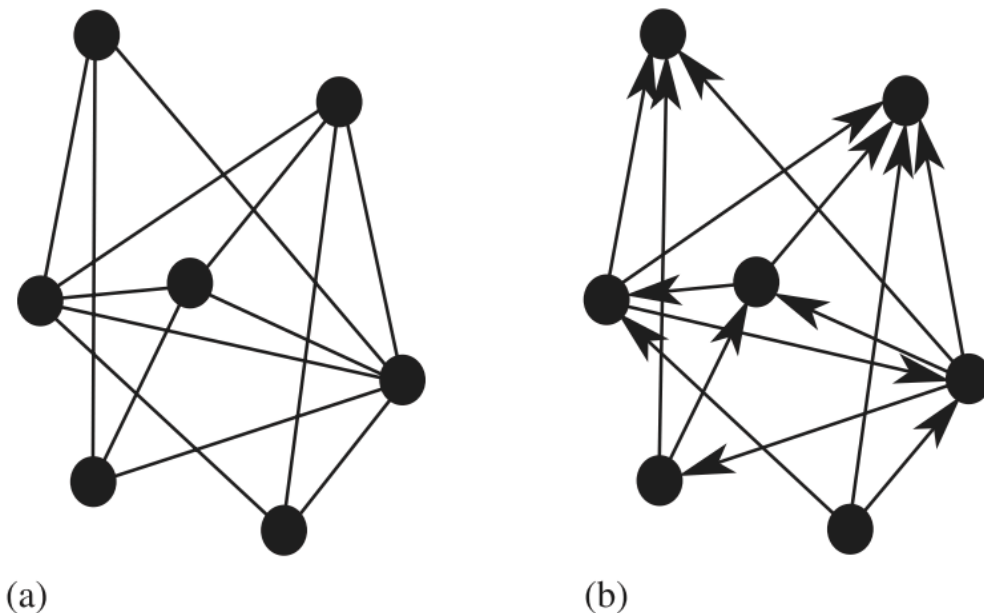


Figure 2. Representation of an undirected network (a) and directed network (b). Network with 7 nodes and 14 edges. In directed networks adjacent nodes are connected by arrows, indicating the directions of each edge. (Boccatelli et al., 2006)

For undirected networks, information on how the degree is distributed can be obtained by a plot of $p(k)$. In the case of directed networks, the degree of the node has two components, outgoing links and ingoing links, then the total degree is defined as $k_i = k^{\text{out}} + k^{\text{in}}$. (Boccaletti et al., 2006)

Geodesic path and diameter

Within networks, shortest paths are relevant in transport and communication, the faster a message is sending the better, that is the main reason for geodesic path, which is the optimal path to connect two nodes, if all lengths are represented on a matrix in which the entry d_{ij} is the length of node i to node j , the maximum value is the diameter of the network. (M. E. J. Newman, 2003)

$$L = \frac{1}{n(n-1)} \sum_{i,j \in N, i \neq j} d_{ij} \quad (2)$$

Where n is the number nodes, L is the geodesic path and d_{ij} is the distance between node i and node j .

Clustering or Transitivity (T)

This means the presence of a high number of triangles on the network. Explained with an example, it means where two nodes with a common node are likely to have connected each other. (Boccaletti et al., 2006) This quantity can be measured by the following equation:

$$T = \frac{3 * \# \text{ of triangles in Network}}{\# \text{ of connected triples of vertices in Network}} \quad (3)$$

Small-world property

When networks have a large size, high number of nodes and edges, it could be easy to think the network will delay sending information, but this property shows that most pairs of nodes in the network are connected by a short path. This short path is calculated with equation 2. It is common that the value of these short paths are much smaller than the number of nodes. (M. E. J. Newman, 2003)

Filamentous fungi network

Fungal kingdom has a sub kingdom named Ascomycetes, which includes yeasts, moulds, and lichens (Blackwell et al., 2007). Some of these organisms are diploid, which's refers they only have one set of chromosomes. Therefore, their reproduction is asexually, and their growth is through filamentous hyphae. These have specialised structures called conidial anastomosis tubes, which connect with germlings and ungerminated conidia (Roca et al., 2005). Thus, forming an interconnected network called mycelia. The mycelial colonies have communications signals inside cellular network, which are used to regulate hyphae growth, periphery of a fungal colony (Jennings, 1984).

Filamentous fungi are multinucleate and needs to build enough space for almost 60 nuclei in hyphal tip cells. This is an advantage because nucleus supply material required for growth. On the other hand, uninucleate yeast cell synthesize proteins from a single gene. Meanwhile, filamentous fungi in the tip cell has multiple copies of the same gene in the same cytoplasm, depending on this number, filamentous fungi may switch their growth phase (Horio, 2007).

The fungi kingdom has the simplest cytoskeleton organisation among all eukaryotes (Mineyuki, 2007) and contain extensive actin cable network in the cytoplasm (Heath, 1990) which get enriched at the tip region and the site of septum formation (Akashi et al., 1994).

Filamentous fungi growth

As was stated before, Ascomycetes have a growth system of branching tubes called hyphae, which have a specialised unidirectional growth pattern called tip growth (Harris & Momany, 2004). Inside hyphae can be found the Spitzenkörper, cytoskeleton, and apical dome. The mycelium is constructed by apical extension, branching, and anastomosis (a process where hyphae fuse), resulting in a structure similar to a nest of interconnected tubes.

The mycelium of ascomycetes is homokaryotic when the hyphae grow from the germination of a single uninucleate spore, and the nuclei in the mycelium are genetically identical. On the other hand, some ascomycetes have heterokaryotic mycelia. This is produced by anastomosis with another fungi mycelium or by nuclei altered in cell division stage due to nutrients availability. Another common condition about nuclei is the dikaryotic mycelium, where each cell contains two genetically distinct nuclei. To distinguish dikaryotic with monokaryotic mycelia, the septa must be analysed. If the septa are perforated and allow the exchange of cytoplasm and organelles, then the mycelium is dikaryotic. This property is common on Basidiomycetes and Ascomycetes, which together constitute the subkingdom Dikarya. (Webster, 2007).

Additionally, the mycelium is constructed by a network of hyphae. The hyphae are made by septa or cross walls, which is a structure made by side-to-side cells, sharing nuclei, organelles and plasmids. (Webster, 2007).

Through maturation, the hyphae create conidiogenous cells, which oversee asexual reproduction. The spores or conidia in ascomycetes have several steps in the production and release mechanisms of them. Some of the main processes are conidiogenesis, maturation, delimitation, secession and proliferation of the conidiogenous cell. (Webster, 2007).

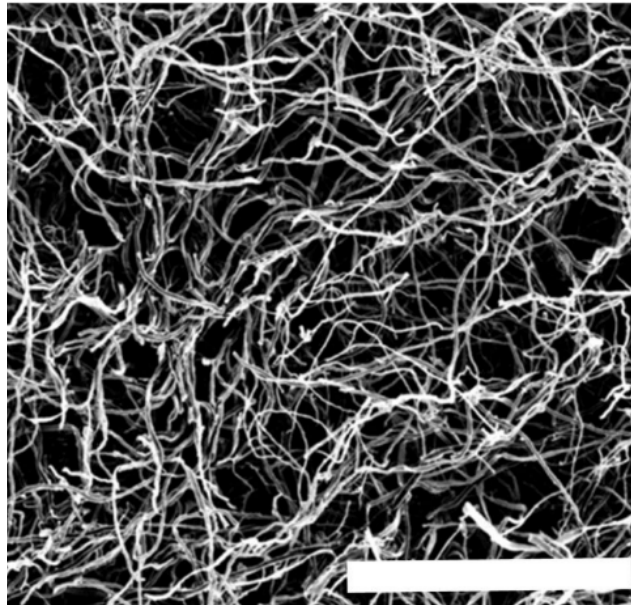


Figure 3. Micrography of filamentous fungi network of *Trichoderma atroviride* observed with a Scanning Electron Microscopy. Scale bar 100 μm (Islam et al., 2017).

Hyphae

As was stated before, hyphae are the principal constituents of mycelium. Accordingly, to H. M. Ward, hyphae have two fundamental properties, the polarity of both growth and secretion of degradative enzymes. Where the enzymes are used to degrade plant cell walls. Meanwhile, the growth has a directional path marked by the nutrients. (Webster, 2007).

The structure of a hyphae is constituted by Spitzenkörper or apical body, cell wall and cytoskeleton. The Spitzenkörper is a region on the tip hyphae with an intense bioenergetic activity where is a rich-nutrients zone, as shown Figure 4. The cell wall is made by chitin, glucans, protein, and lipids. These materials are organized in the Spitzenkörper to create the cell wall. On the other hand, the cytoskeleton is made mainly by microtubules and actin filaments; intermediate filaments do not take place in these microorganisms. (Reynaga-Peña & Bartnicki-García, 2005).



Figure 4. Transmission electron microscopy of a hyphal tip of *Fusarium acuminatum*. Spitzenkörper is in the tip. The black arrows are pointing out the organelles with construction material. (Weber, 2007)

The mitochondria move continuously along the hyphal axis with an average velocity of 0.6 $\mu\text{m/s}$, moving in and out of apical dome interacting with the Spitzenkörper. Also, spherical vesicles move in the same way as mitochondria but traversing long distances with an average velocity of 1.5 $\mu\text{m/s}$. (Ma et al., 1996).

The hyphae elongation or growth is carried out by hyphae maturation, where the Spitzenkörper moved forward keeping a constant distance from the apical pole. Elongation contains a process of contraction preceding apical branching. Is a sudden, synchronised, directional-forward movement of intracellular components, it last 1 second and after the contraction, organelles came back to their normal activities (Reynaga-Peña & Bartnicki-García, 2005). The frequency of contractions varied in various fungi, but for *Trichoderma atroviride* 25% cells showed contractions in more than 3 hours. (Reynaga-pen, 1997).

The cytoplasmic contractions produce morphogenetic consequences like bulges formation in the hyphal profile, and the initiation of subapical or apical

branching. After contractions, the Spitzenkörper disappear by the size reduction and the growth stops, but 3 minutes later a new Spitzenkörper is formed and growth process continues with subapical branch initiation (Reynaga-pen, 1997).

Model system: *Trichoderma atroviride*

Among fungi kingdom, there are versatile species, like *Trichoderma* species, these are found in soil, dead organic matter. Also, they are in symbiosis relationship with other organisms, specially plants, where they are commonly used for control of plant diseases caused by bacteria, other fungi and nematodes (Mendoza-mendoza et al., 2016). Some *Trichoderma* species are capable of parasite Ascomycetes and phylogenetically close species, this is why they are special (Druzhinina et al., 2018). *Trichoderma* species grows through branches called hyphae, which connects with other hyphae to build a filamentous fungi network known as mycelia by a process called anastomosis. Accordingly, with Kubicek, there are 13 *Trichoderma* species commonly found in soil samples, one of them is *Trichoderma atroviride*.

As was stated before, filamentous fungi are asexual, they produce spores with a system called conidia, which is located on hyphae and *Trichoderma atroviride* is not the exception (Steyaert et al., 2010). Conidiation process could be triggered by several stimulus such as light exposure, mycelia injury, pH variation, temperature or any external perturbation considered a treat. Also, these stimuli travel into the network as a chemical signal to produce a reaction. According to Islam (2017), the mechanics of filamentous fungi are not studied yet, and signals propagation must be a priority to try to understand how a signal is transmitted inside a network, but first the network properties must be measured.

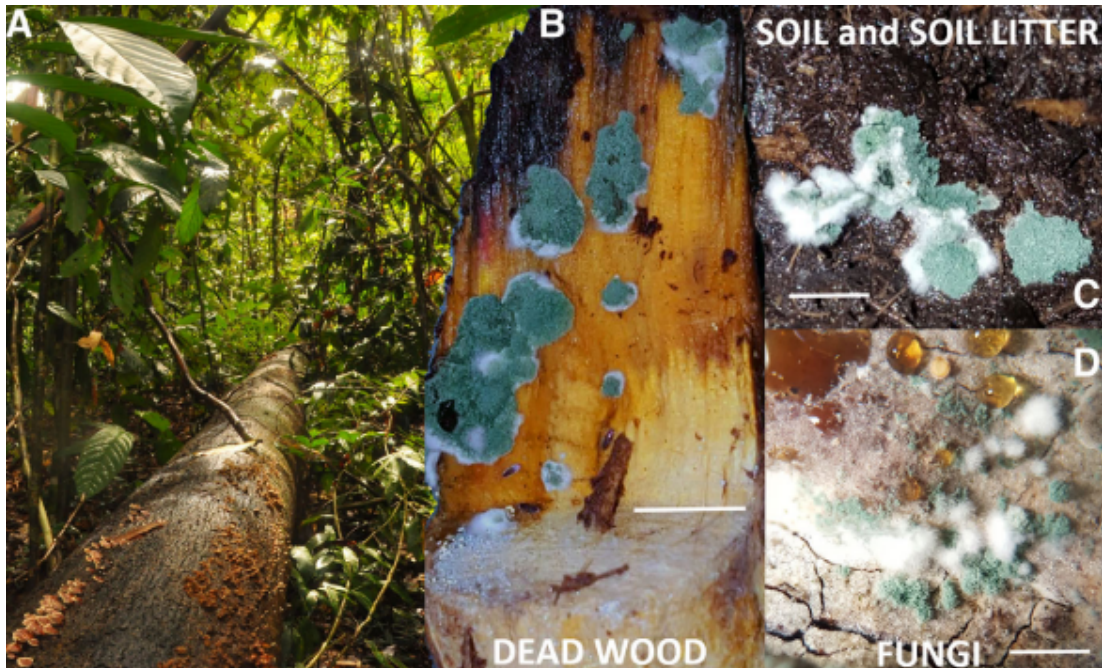


Figure 5. *Trichoderma* spp. in nature. A) Fallen dead wood colonized by fungi. B) *Trichoderma atroviride* on dead wood. C) *T. harzianum* in soil. D) *T. simonsii* on the sporocarps of *Stereum* spp. (Kubicek et al., 2019).

G – Hyphal Growth Unit

According to Trinci and Caldwell, the hyphal growth unit is described by the following equation. (Trinci, 1973)

$$G (\mu\text{m}) = \frac{\text{Total hyphal length } (\mu\text{m})}{\text{Number of hyphal tips}} \quad (4)$$

Mycelium can grow exponentially, but with a same specific growth rate, this is related with the number of hyphal tips and the total length of mycelium. Therefore, *G* could show if the mycelium grows at the same rate. (Trinci, 1973). Also, there was no concept of a *G* incorporated in the model, so instead it arose because of local branching and anastomosis rules. However, *G* may be a useful statistic from which to quantify and describe the response of a mycelium growing in a particular environment, but it is not sufficient to describe dynamics of a fungi. (Boswell & Hopkins, 2008)

However, recent studies in fungi growth rate use the G number to analyse and compare growth rates of filamentous fungi and their mutants, as show Withers and her team. They have grown *Aspergillus oryzae* with glucose-limited chemostat and four morphological mutants were recognized, then the G number has been calculated respectively. The conclusion was that the degree of branching of mycelia is a determinant of culture viscosity and influences the macroscopic culture morphology. (Withers et al., 1994). On the other hand, an experiment from Boswell shows that there is a transient phase where G initially increases before declining toward a limiting value. (Boswell & Hopkins, 2008).

The G value of *Trichoderma reesei* and *Aspergillus oryzae* are presented in Table 1.

Table 1. G values of different filamentous fungi. All fungi were incubated in solid agar. *A. oryzae* were compared with its own mutants' strains.

Filamentous fungi	G (μm)	Ref.
<i>A. oryzae</i>	208 ± 8	(Booking et al., 1999)
<i>A. oryzae (HNV8)</i>	133 ± 11	(Booking et al., 1999)
<i>A. oryzae (UVb33)</i>	172 ± 9	(Booking et al., 1999)
<i>A. oryzae (Parental strain)</i>	192 ± 8	(Withers et al., 1994)
<i>A. oryzae (Flat mutant)</i>	273 ± 21	(Withers et al., 1994)
<i>Trichoderma reesei</i>	60 ± 20	(Lejeune & Baron, 1997)

Our work

In this project we propose the extraction of complex network parameters of filamentous fungi network of *Trichoderma atroviride* to analyse how this biological network can behave like a complex network throughout mycelium. To achieve this, first, was needed to grow the mycelium with a standard process, without background inhomogeneities, incubation time and size. Secondly, collect images from the mycelium with a bright-field optical microscope, then assemble them to create an image with the entire mycelium. Finally, extract networks parameters using the

software NEFI, such as number of nodes, edges, total and average lengths, and statistical analysis.

Hypothesis

The mycelium of *Trichoderma atroviride* has a complex network structure because it has the basic elements of a network, nodes, and edges, which over time increase to a more intricate conformation.

General goals

To establish the basic conditions of cultivation of *Trichoderma atroviride* mycelium and methodology for the study of structural complex networks in this organism.

Specific goals

- i. To grow *T. atroviride* mycelium at different times from mycelia in culture and by germination of individual spores for study at the microscopic level.
- ii. Segment and binarize the images obtained by optical microscopy using digital image processing in order to retain the mycelium of the filamentous fungus.
- iii. To record the different network parameters of the filamentous fungal mycelium in terms of nodes and edges in order to analyse the development as a function of time based on the structure of a complex network.

II. Research methodology

In this chapter, it will be explained the procedure to fulfil the goals presented in the previous chapter. The first goal, mycelium growth, two methods will be tested to get a mycelium in the properly conditions to this project, the main conditions are clean images, high contrast between agar and hyphae, germination time and mycelium size. The methods that will be described are stab and surface spread culture. Also, other variables will be taken in consideration, such as agar volume for a correct acquisition of images, number of spores to analyse a single mycelium and incubation time to control the size of mycelium.

Once the mycelium has grown, the second goal must be achieved, picturing the filamentous fungi with a bright-field optical microscopy, with a 80x and 200x lens, but the vision field were not enough to photograph complete mycelium, therefore, it will be presented the procedure to capture images. Also, it is required for the next stage that images need to be binarized, this process made with ImageJ, which is described step-by-step, and is called pre-processing. Finally, pre-processed images are going to be assembled into a mosaic to have a complete mycelium ready to extraction with an image manipulation program GIMP. Additionally, some pictures acquirees error through the three processes, to fix these problems it is used the brush tool of GIMP.

As a third goal, the extraction of the network from mycelium will be completed with a specialized software named NEFI. This program uses a pipeline to extract networks parameters such as length, coordinates, and grade nodes. The pipeline is set up with five categories and each has a list of algorithms to do specific task in order to extract the network parameters. Once the extraction is complete, NEFI throws a carpet with images and lists. Therefore, this data will be analysed and selected to extract the network parameters such as grade nodes, average grade nodes, total length, average length and so on.

Mycelium growth

For both methods described before, it was started with the ceparium creation, where the storage spores were inoculated in a Petri Dish with Potato Dextrose Agar (PDA) from Sigma Aldrich. The process were 4 cycles of 24 h of incubation at 27° C in darkness with 15 minutes at sunlight exposure every day, to produce mature spores which are going to be expressed in conidiation halos. Also, following this methodology an experiment to know the behaviour of the fungus was carried out, to provide information about spore's maturation, with the goal to increase the mature spore production in our cepariums.

For all procedures, it was used alcohol (99%) to clean the work area and 3 – 8 alcohol lamps were lit as the cleaning of the table was done. According to the Mexican standard NOM-111-SSA1-1994 the medium conditions are pH of 3.5, 39 grams of PDA (Sigma Aldrich) per litre of distilled water and prepared in a sterilized zone following the manufacturer instructions.

Two methods of inoculation were used. First, stab culture method was carried out with an inoculation fungal loop, where it was subtracted a bunch of spores and deposited into the centre of the PDA to finally, incubate in darkness at 27° for 10 h, 11 h, 12 h, 13 h and 24 h. This experiment helps to detect the mean problems of mycelium growth.

Secondly, the surface spread culture was carried out as follows; a bunch of spores were collected with needle bevel from the ceparium to disperse them in 1 mL of water with a vortex for 1 minute, this is the solution "P" with an unknown concentration of spores. Solution "P" was used to create 3 more solutions with different dilution factors in 1 mL, taking 20 μ L of "P" to 1:50, 10 μ L for 1:100 and 1 μ L for 1:1000. Then, these 3 solutions were dispersed with a vortex for 1 minute each one. Next, these solutions were used to inoculate Petri dishes, taking 20 μ L of one dilution to be added into the PDA, then 5 to 10 glass beads were used to disperse the volume for all the area and then the beads were removed. Finally, Petri dishes were covered with aluminium and incubated at 27 °C for 37 h, 40 h and 43 h. This experiment was fivefold for each hour previously established.

Spore's germination

In order to determine the time of spore's germination a simple experiment was carried out, where six petri dishes were incubated following the described methodology in this section. Then, one petri dish was observed every two hours after 24 hours of incubation, observing at 24 h, 26 h, 28 h, 30 h, 32 h and 34 h after incubation started. Through observation, the germinated spores were counted, plotted, and fitted with a sigmoidal curve.

Brightfield optical microscopy

Once the mycelium grows in the incubation time. It was observed with a T370B-3M brightfield optical microscopy of AmScope. This microscope has four objective lenses with the following magnifications 80x, 200x, 400x and 800x. The images were recollected with a MU300 camera coupled into the microscope, supported by a software of the same trademark.

The set scale for images were 635 pixels for 1 millimetre in the case of 80x, which was the principal lens used. Also, images were captured with a 200x lens when the 80x lens could not define between two very close hyphae or the appearing of black spots in the intersection of two or more hyphae.

Image acquisition and processing

The images were taken by an optical microscope with a digital camera controlled by the software AmScope in the highest camera pixel resolution (2048 pixels x 1536 pixels) with an 80x objective lens. In all cases, the mycelium was bigger than the field vision of the objective, to solve this problem several pictures were taken in different parts of the mycelia. Then, images were used to assemble them digitally as a mosaic.

Digital processing

On this stage, once we had got the images of mycelia, different digital adjustments had been applied in order to binarize and extract the network. To extract the network from the images, the process was divided in three stages; stage one consists in pre-treatment, second stage is the mosaic assembly, and third stage is made by NEFI processes.

The pre-processing consists in a seven-step process made with the digital free license software ImageJ, said process transform originals images (Figure 6) into binarized images (Figure 13). Original images have lightning variation zones due to the interactions of the medium with the microscope light. Also, have several trash particles attributed to the medium or the solution P, which has rests of the mycelia and not only spores. Furthermore, some original images show two or more hyphae so close to each other that it is not easy to distinguish a separation. For these original

image's characteristics, the binarization process is needed, because it is necessary to work with images with no trash, lightning variation zones and indistinguishable hyphae.

Pre-processing steps

1. Greyscale

Every image was converted into an 8-bit image in greyscale to reduce the size file and avoid chromatic effects derived from light and medium interactions. *Image > Type > 8-bits*

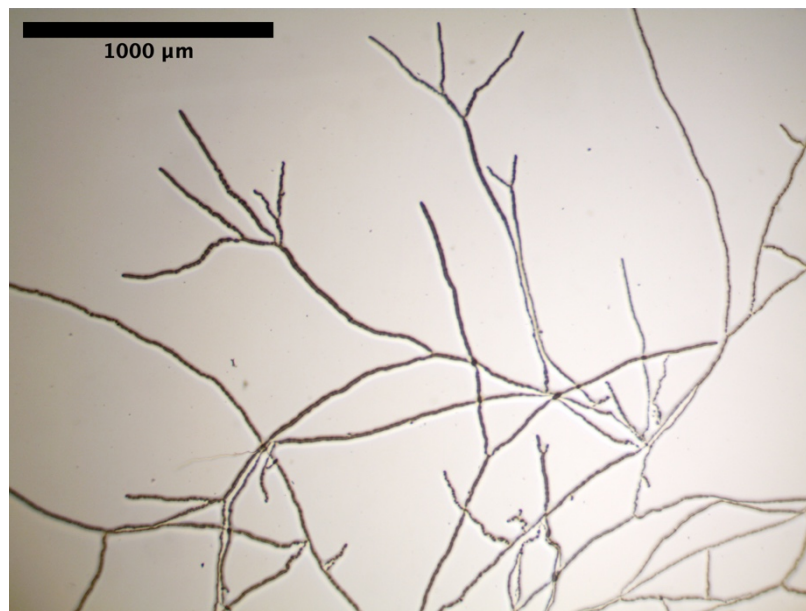


Figure 6. Image of a section of *Trichoderma atroviride* mycelium, obtained with an optical microscope with 80x lens, after 40 h after incubation or 11 h after spore's germination. Initial image.

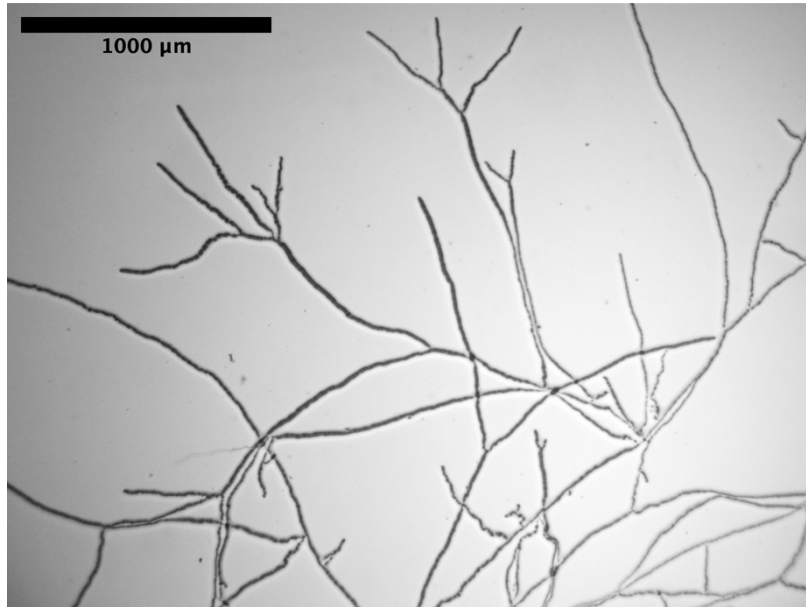


Figure 7. Transformed image into an 8-bit format of Figure 6. First step in pre-processing.

2. Brightness and contrast

This adjustment is used to increase pixels values, in order to obtain images with higher contrast between hyphae and medium. Also, it allows us to homogenize the background indirectly. *Image > Adjust > Brightness and contrast*

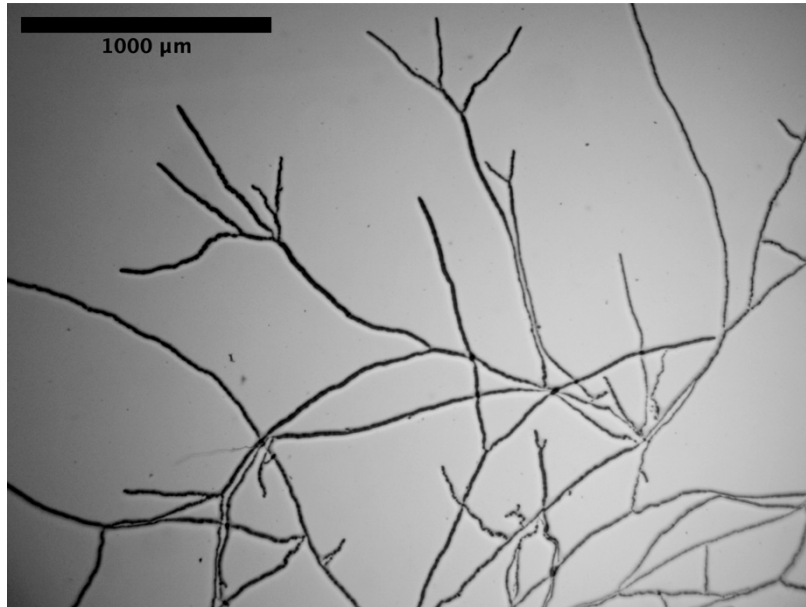


Figure 8. Second step in pre-processing, an adjustment of brightness and contrast was performed onto Figure 7.

3. Gamma adjustment

As we can see in Figure 8, the background is still inhomogeneous, if this step is skipped some black stripes will appear accordingly to the lightning variation zones when the threshold is applied. Furthermore, this step is necessary to homogenize the pixels intensity in the background. Also, this process does not affect in major way the hyphae pixels intensity. *Process > Math > Gamma*

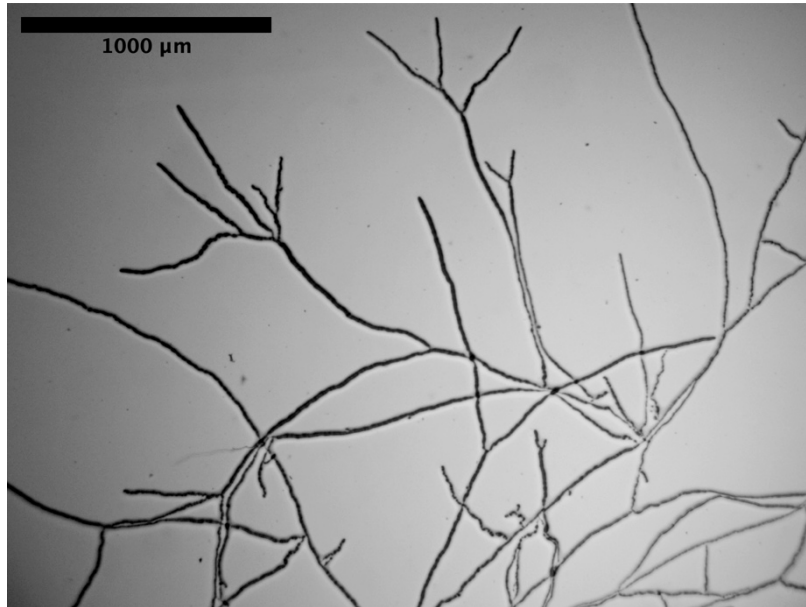


Figure 9. Third step in pre-processing, a gamma adjustment is applied in Figure 8.

4. Subtract background

Once the image has a homogeneous background, the next step is removing it to have only the pixels that conform the hyphae. This process is carried out by removing the pixels with certain intensity and this is done by establishing an intensity range. This process may affect in a minor way the outer zone of the hyphae, creating a low distortion in the zone previously described. *Process > Subtract background*

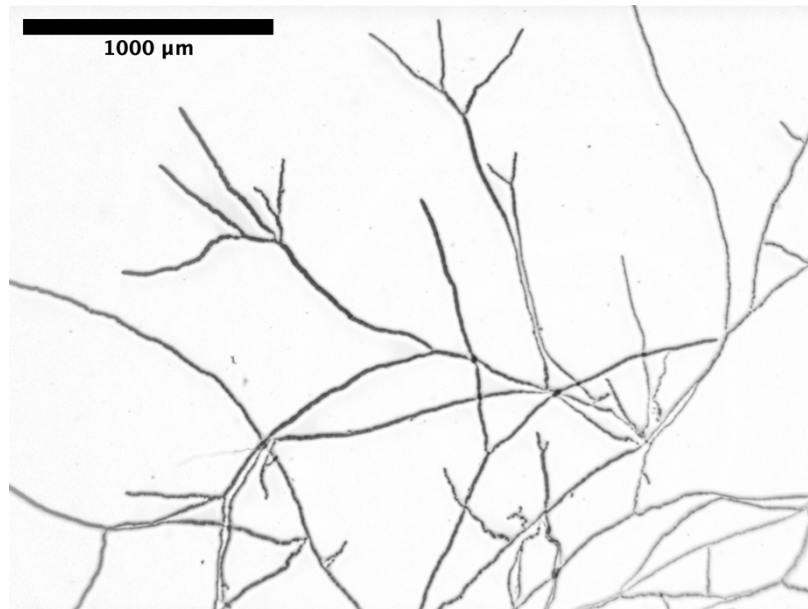


Figure 10. Forth step, the background was subtracted from previously figure.

5. Threshold

After removing background, once the range of intensities between the pixels that conform the hyphae and the background is very large, the threshold is applied to be able to segment the image into two groups, black and white. The colour white is attributed to the highest intensity pixels, meanwhile, the lowest intensity pixels will be black. *Image > Adjust > Threshold*

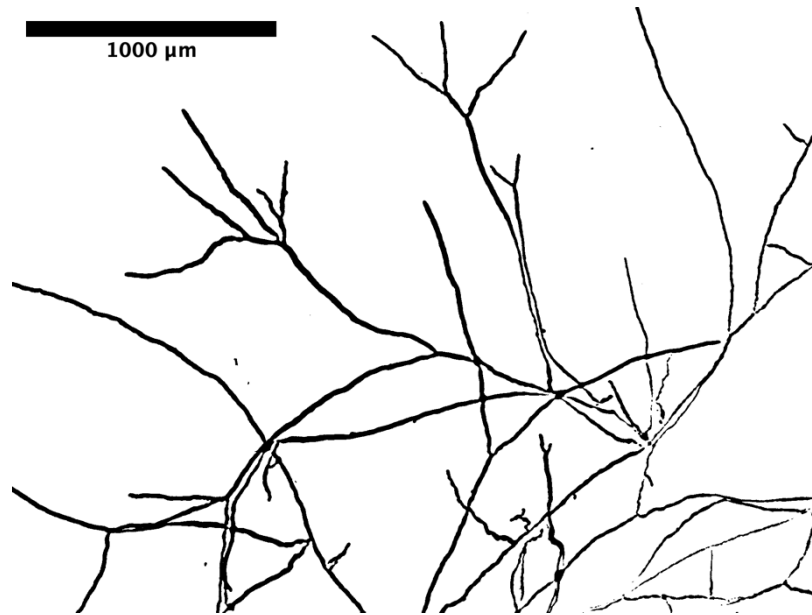


Figure 11. Fifth step, a threshold is applied once the background is subtracted.

6. Binarize

After applied the threshold, some pixels could not be changed into a white and black format, so it is needed to convert all pixels into this format applying this function.

Process > Binary > Make binary

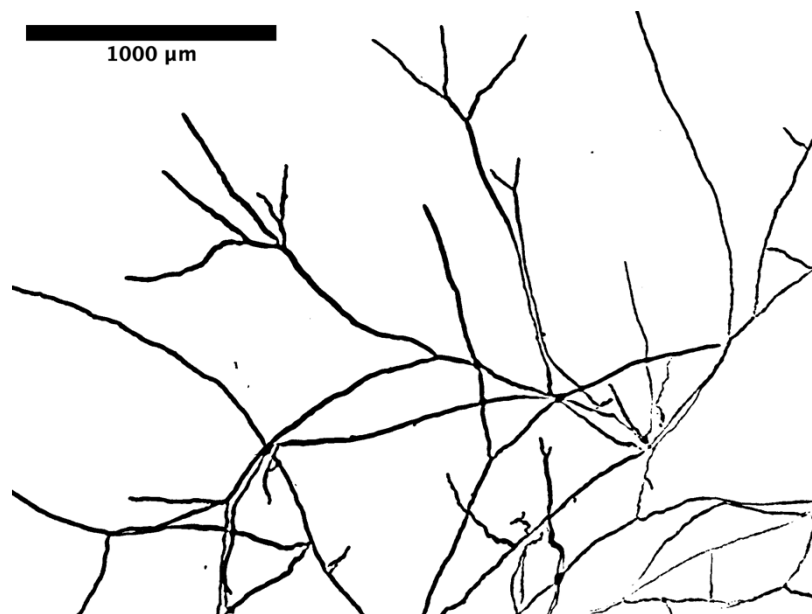


Figure 12. Sixth step, binarize the image, in order to have only two values of pixels, 255 (black) and 0 (white).

7. Particle removal

After all processes, it could be the presence of black spots belonging to trash in the medium, lens error or even lightning variations, because of these, it is required to remove all small and big black spots. ImageJ has a function to do this with three options set up, first, it must be chosen the area in pixels to be erased, second, the shape of the spots and third, choose what to do when the program finds these spots. Once the spots are detected a new image will be created only with the spots and using an image calculator it can subtract the spots from the original image. In this way, we finally get a binarized image with the mycelia network. *Analyze > Analyze particle > Set up particle size*

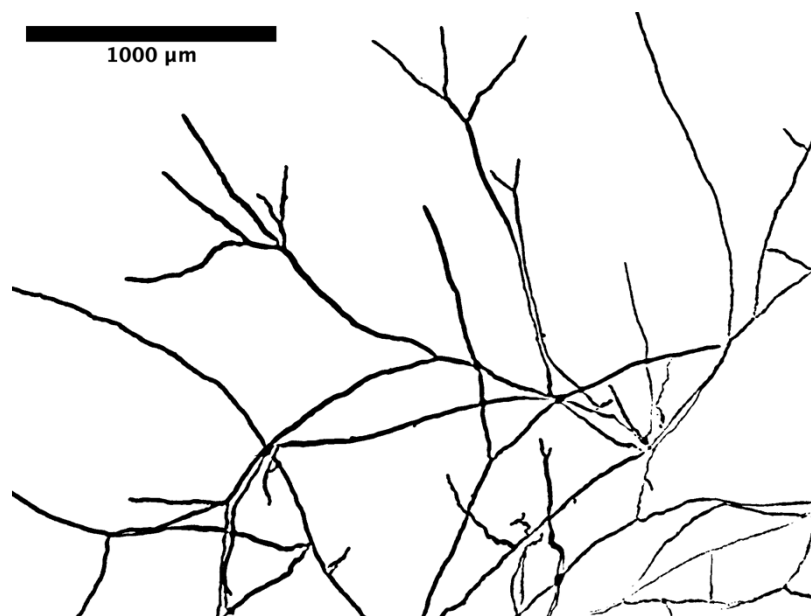


Figure 13. Sometimes, black spots appear due to threshold or are trash from medium, it is necessary to remove them, an ImageJ tool was used to achieve the remotion.

All the images are pre-processed and after this they are ready for the next stage.

Mosaic assembly

After pre-processing, images were assembled to reconstruct the mycelium, due to microscopes field of view is not enough to capture it all in one shot. However, all captured images present areas with heterogeneous focus, affecting the final image, as shown in Figure 13. Several images were captured adjusting the focus area to be able to perform the assembly more accurately, but this increases the number of images to assembly and some of them had to be cut with the software used.

The assembly was made with GIMP, a free license program. This program opens the images as superimposed layers allowing is to accommodate one by one following the branching of the hyphae. The arrangement is done by decreasing the opacity of upper layer at 50 %, which allows us to see through it. Then, hyphae are matched between both layers, taking care not to create distortions in the image. Once the hyphae are correctly superimposed, the opacity is restored at 100 %. Finally, both layers are merged into one image. This process is shown in Figure 14 and 15. In addition, the final image size depends on the size of mycelia but approximately the size is around of 4500x3800 pixels. (Dikec et al., 2020)

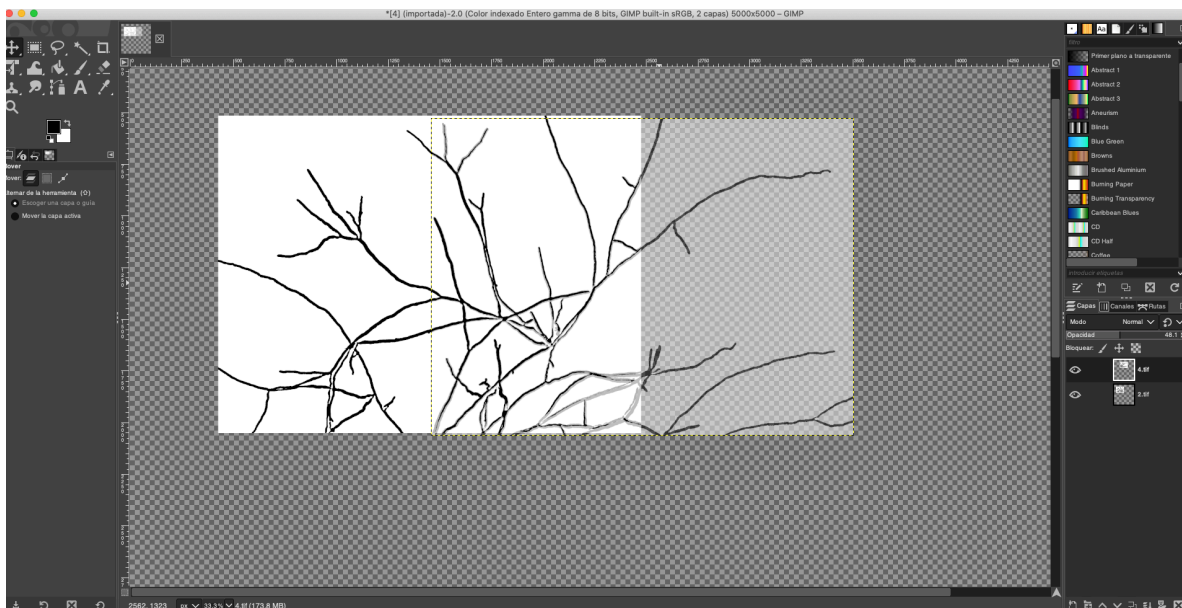


Figure 14. Screenshot of mosaic assembly, images were opened as layers, the left layer has 100% of opacity, right layer has 50% of opacity, to overlap and match the hyphae.

Once the mosaic was completed, pre-processing left exposed pixels in the hyphal contours, which could be recognizable as nodes, increasing the number of real nodes. To fix this, a manual smoothing was carried out in the contours, using the “brush tool” function of GIMP. Also, this tool was used to separate hyphae that were joint by the pre-processing.

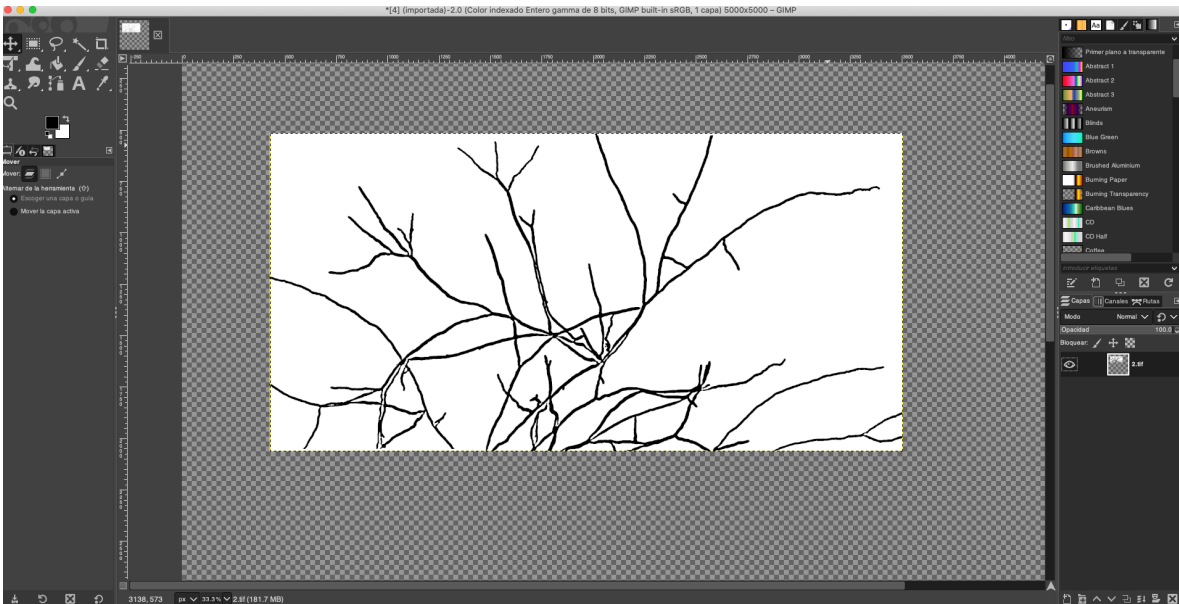


Figure 15. Layers of previous figure combined as one, with matched hyphae and 100% of opacity for both layers. In this way, mycelium has been assembled into one single image.

Network extraction

For this stage, it was used a software called “Network Extraction From Images” (NEFI) developed by Max Planck Institute for Informatics. (Dirnberger et al., 2015). This program recognizes, identifies, and extracts the network with a pipeline, conformed by 5 categories, and every category has its own algorithms. The categories are pre-processing, segmentation, Guo-Hall Thinning, Guo-Hall Detection and Guo-Hall Filtering. NEFI runs the pipeline in order, so it is important to follow the sequence previously mentioned to have a successful result. The pipeline used in this project was the following: Segmentation “Watershed DE Otsus”

> Thinning “Guo Hall Thinning” > Detection “Guo Hall Detection”. The process showed before have the following structure: Category “Algorithm”.

Once NEFI extracted the network, use blue squares to select nodes and red lines for edges. It may be possible that lengths are associated to these red lines than the hyphae, in this sense the lengths proportionated from NEFI are an approximation.

```

#D:\Downloads\nefi-windows_64bit_build\nefi-windows_64bit_build\NEFI.exe
# GMT Wed Jun 16 00:07:31 2021
#
(2456, 2718)|3
(2486, 2740){'width_var': 6.3125, 'pixels': 32, 'width': 6.0, 'length': 41.870066}
(2488, 2802){'width_var': 3.9051870748299318, 'pixels': 84, 'width': 6.8928571428571432, 'length': 103.39698800000002}
(2410, 2593){'width_var': 5.4575360000000019, 'pixels': 125, 'width': 10.592000000000001, 'length': 146.05384400000003}
(120, 2291)|1
(909, 2516){'width_var': 0.97936294518578493, 'pixels': 789, 'width': 10.47401774397972, 'length': 894.13928600000011}
(3297, 2873)|1
(3260, 2138){'width_var': 2.997245179063361, 'pixels': 66, 'width': 13.181818181818182, 'length': 84.15434600000003}
(2524, 2603)|1
(2481, 2613){'width_var': 9.3250405624661958, 'pixels': 43, 'width': 7.9767441860465116, 'length': 49.14214}
(678, 1382)|3
(612, 1373){'width_var': 3.9753846153846149, 'pixels': 65, 'width': 11.199999999999999, 'length': 74.45585200000002}
(953, 1765){'width_var': 2.7984204979903926, 'pixels': 404, 'width': 14.626237623762377, 'length': 511.2103559999988}
(670, 1366){'width_var': 2.984375, 'pixels': 16, 'width': 11.875, 'length': 21.313712}
(4915, 1839)|3
(1809, 1897){'width_var': 0.86982248520710059, 'pixels': 26, 'width': 8.2307692307692299, 'length': 31.313712}
(1894, 1864){'width_var': 1.4722222222222221, 'pixels': 30, 'width': 6.833333333333333, 'length': 38.627424}
(1932, 1832){'width_var': 1.37109375, 'pixels': 16, 'width': 12.5625, 'length': 20.899498}
(1313, 2768)|3
(1308, 2773){'width_var': 0.5599999999999994, 'pixels': 5, 'width': 25.199999999999999, 'length': 9.899498000000001}
(1319, 2771){'width_var': 3.5833333333333335, 'pixels': 6, 'width': 22.5, 'length': 9.656856000000001}
(1327, 2735){'width_var': 10.370982552800733, 'pixels': 33, 'width': 20.515151515151516, 'length': 40.798996}
(1036, 2137)|3
(1079, 2176){'width_var': 2.2544137618832059, 'pixels': 47, 'width': 8.8510638297872344, 'length': 63.911704000000015}
(962, 2300){'width_var': 0.99070263679317172, 'pixels': 162, 'width': 11.506172839506172, 'length': 195.06605000000008}
(1034, 2129){'width_var': 2.984375, 'pixels': 8, 'width': 16.625, 'length': 11.242642}
(1359, 2271)|3
(1322, 2493){'width_var': 1.837289926953985, 'pixels': 222, 'width': 10.797297297297296, 'length': 256.72290600000001}
(1261, 2292){'width_var': 3.906897651185036, 'pixels': 97, 'width': 10.896907216494846, 'length': 109.35535000000002}
(1495, 2089){'width_var': 0.8763151809457741, 'pixels': 186, 'width': 11.672043010752688, 'length': 243.50467600000013}
(2802, 2244)|3
(2793, 2242){'width_var': 4.666666666666667, 'pixels': 9, 'width': 15.0, 'length': 12.656856000000001}
(2875, 2199){'width_var': 1.6103395061728394, 'pixels': 72, 'width': 12.027777777777779, 'length': 93.05384400000003}
(2898, 2634){'width_var': 2.9517685733070347, 'pixels': 390, 'width': 11.805128205128206, 'length': 440.46303799999924}
(2326, 1803)|4
(2126, 1975){'width_var': 4.5932784636488337, 'pixels': 216, 'width': 10.407407407407407, 'length': 282.6173839999999}
(2326, 1800){'width_var': 0.0, 'pixels': 2, 'width': 16.0, 'length': 4.828428000000001}
(2327, 1802){'width': 11.346320346320347, 'length': 258.26705399999996, 'width_var': 3.1094994471617849, 'pixels': 231}
(2364, 2264){'width_var': 5.5596105796603625, 'pixels': 461, 'width': 13.006507592190889, 'length': 500.69347399999947}
(257, 232)|1
(754, 624){'width_var': 1.5610504923955484, 'pixels': 524, 'width': 9.5438931297709928, 'length': 677.1881099999996}
(2019, 1641)|3
(2034, 1646){'width_var': 1.5357142857142858, 'pixels': 14, 'width': 13.5, 'length': 18.07107}
(1990, 1663){'width_var': 4.5752551020408161, 'pixels': 28, 'width': 8.8214285714285712, 'length': 39.112708}
(1935, 1607){'width_var': 5.0011890606420941, 'pixels': 87, 'width': 8.4137931034482758, 'length': 102.25484800000001}
(2089, 2084)|3
(2062, 2092){'width_var': 3.609467455621302, 'pixels': 26, 'width': 8.0769230769230766, 'length': 32.14214}
(2082, 2070){'width_var': 1.1683673469387759, 'pixels': 14, 'width': 9.7857142857142865, 'length': 18.899498}
(2147, 2709){'width_var': 3.0902937599999998, 'pixels': 625, 'width': 11.6432, 'length': 692.03159799999998}
(2453, 3019)|1
(2473, 2873){'width_var': 2.1227247138299865, 'pixels': 146, 'width': 7.7123287671232879, 'length': 159.18377800000002}
(2701, 1526)|3
(2700, 1522){'width_var': 0.0, 'pixels': 4, 'width': 12.0, 'length': 6}
(2530, 1515){'width_var': 2.1354114424507812, 'pixels': 161, 'width': 5.1614906832298137, 'length': 172.11270800000003}

```

Figure 16. Screenshot of NEFI data list. This list has the coordinates of nodes and the lengths of edges and widths of edges. The data was filtered to only use the coordinates, lengths and degree nodes.

Also, some edges and nodes could not be recognized because the program does not find an end to a particular line of pixels, thus, the images resulting from the assembly must have a white background frame to identify hyphae. The response speed depends on images size, this is specified by the developers on its website.

After the extraction, NEFI returns a set of images, each one corresponds to a category of the pipeline, so one can analyse every step of the network extraction. Additionally, NEFI creates a folder with these images, the pipeline used and the extraction data. This extraction data consists in a list with the nodes, edges lengths, edges widths and coordinates, as shown in Figure 16. (Dirnberger et al., 2015)

NEFI stages

1. Pre-process

This process applies filters to increase the contrast in images. However, this part of the process does not erase black spot and image imperfections, for this reason this category was not applied into the images. This section has the following algorithms, bilateral, blur, colour enhance, FM denoise, FM denoise colour, Gauss Blur, Image reduce, invert colour and median blur.

2. Segmentation

In this category, NEFI applies a filter to exchange the pixels value, in order to prepare the image to the most important part. This section has several algorithms to use but only two will be used, there are Watershed DE Otsus and Grabcut DE Otsus, both work at the same way. First, they invert the pixels values, white pixels are turned into black and vice versa, to use them as a topographic image, something like a riverbed, where high pixels values are the walls that contain the river, and white pixels or low value pixels are the river. In this stage of the pipeline, it is important to have a clean image because every free pixel could be considered as a node, and this introduces an error in our further analysis.

3. Guo-Hall Thinning

Thinning or skeletonization is the most important step in the network extraction, this category only has one option Guo-Hall thinning algorithm. It makes a thinning of white pixels until they have a line one pixel thick, this is applied in all white lines.

Also, in this part the algorithm has mistaken with nodes of 4 or high degree, because the thinning results in a non-symmetric cross causing the program to detect more nodes than there are.

4. Guo-Hall Detection

Once the thinning is done, the algorithm of this section takes place, at this part of the process the last two steps are key to find nodes and extract the network, both creating the ideal conditions to detect nodes. The detection algorithm is carried out by sensing the space surrounding the pixels. First detect a white pixel surrounded by three black pixels and one white pixel forward, the program detects it as a node of degree one. After, the algorithm moves forward over the new white pixel, two scenarios could present. If this white pixel is surrounded by a black pixel at each side and one white pixel forward and backward, then the algorithm does not mark a node and gives another step forward. If the white pixel is surrounded by three white pixels (one backward, another forward and the last one at one side) and one black pixel, then is marked as a node of degree three. This process is repeated until no more white pixels appear. For degree four nodes, the process is similar, just finding a pixel surrounded by four white pixels. Also, it is important to add, that higher degree nodes are difficult to detect by the algorithm, for this reason the procedure to detect them in manual way.

5. Guo-Hall Filtering

This is the last stage of the process and was not used. This category has the following algorithms: connected component, edge attribute, keep only LCC, simple cycle and smooth 2 nodes. The previous algorithms help to erase isolated nodes from the analysis but did not do it from the images, that is why it was not used.

Statistical Analysis

As was stated before, NEFI created a folder with network extraction information. This folder contains quantitative and visual data. The quantitative data has a list with

coordinates, lengths and a number associated with the nodes. Where, the last one, is believed to represent the node degree. But, in so many cases it seems not be correct, because it acquires 0 or 2 as values and these are not possible in this network. Nodes with 0 values means an isolated node, which are not presented. On the other hand, nodes with value of 2 are corners, but hyphae do not create them. Then, the full list was analysed. Filtering the data by coordinates it was found that every coordinate follows a conditionate rule. Where, if only one row appears, it means that number is the node degree. But, if the coordinate shows more than one row, they are the node degree and the edges connected to it. Therefore, when adding the number of edges with the value of the first row we obtain the node degree.

On the other hand, visual data contain images from each category of the pipeline; segmentation, thinning and detection. The first two are control images of the process, where the user of NEFI can check them and verify the performance of the pipeline. The last one contains the blue squares and red lines on the mosaic, which help us to probe the conditionate rule proposed for the node degrees. Using ImageJ, the nodes were located on the “detected mosaic” with the coordinates of the quantitative data. Afterwards, it is visually confirmed that a node has the degree or the number of connections that quantitative data established before. Once the node degrees are subtracted two network parameters are calculated, “n” number of nodes in the network and “k” the average degree of nodes in the network.

Another issue detected involves the lengths which were presented by NEFI in pixels. To solve this, the relation described in Brightfield optical microscopy was used, converting all the lengths in micrometres to obtain two parameters more, Total Length and Average Length.

For all mycelia these parameters were calculated and grouped into charts. Then, were calculated the average, standard deviation and error standard, in order to plot the parameters mentioned above versus time. To compare length average two quantities were calculated, the arithmetic and exponential average. Therefore, nodes of each mycelium, were separated into their degrees and compared between the three times planted in the experiment, in order to analyse the network evolution.

G – Hyphal growth unit

Once the data were filtered, the total length of mycelia and the node of degree 1, are used to calculate the G value using Equation 4. Then a plot of G vs time will be presented.

As was stated before, this value could help us to describe the growing rate as a complementary statistic parameter to explain the growth of mycelium. As expectation, there are two scenarios. First, the data have similar values, and the plot will be constant, meaning a constant growth rate. The second scenario is where the data have values totally different, making an irregular pattern of the plot.

III. Results

In this chapter, are present the results of the investigation. Where the principal reasons about the change in the inoculation method for mycelium are exposed, which involves the volume agar, incubation time and spore's number. Also, the photo-conidiation process is presented below, describing the effects of incubation and exposure to sunlight. Furthermore, it will be discussed the main drawbacks in image acquisition like contrast and focus zones, definition with close objects and number of images per mycelium. Next, the pre-processing mycelium will be showed after mosaic assembly for the three times selected previously and discussed in order to prepare them to the network extraction. Therefore, the main characteristics of NEFI's extraction are presented where nodes, edges and lengths will be exemplified in figures, then are graphs with the statistical information about the complex network's parameters calculated from the NEFI data. The goal of this procedure is to extract from the assembled images the network complex parameters on time-based of *Trichoderma atroviride* mycelium. Then, show information about the mycelium being a complex network and the behaviour of a biological complex network at the first 14 hours of growth.

Mycelium growth

The first goal to achieve was to know the behaviour of the fungi. Examining the Table 1, it can be appreciated the evolution of mycelia through 4 days with 15 minutes of sunlight exposure every 24 hours. At day 1, after 24 hours of incubation, the mycelia have around 1 centimetre of diameter with a translucent hue and soft appearing. At day 2, the mycelia have 4 centimetres of diameter, with still a translucent hue. The mycelia on day 3 have almost 8 centimetres of diameter and still translucent hue, but now two conidiation halos appeared. The sunlight act as a trigger for conidiation processes, creating spores which at day 3 spores remains immature. On day 4, mycelia have covered the totality of the Petri dish, with 3 conidiation halos, which, in comparison with viewed at day 3, now are green. When the spores are green, they are mature and ready to spread. These were the spores used to inoculate further experiments.(Pinto et al., 2020)

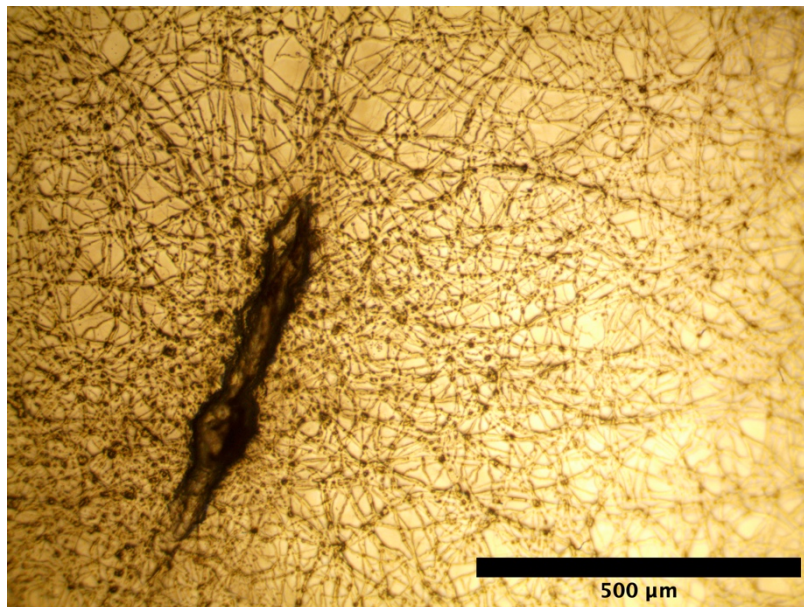


Figure 17. Centre of mycelium after 24 h of incubation, captured with an optical microscope and 200x lens. It is appreciated that the image has a big black spot in the centre, low contrast between hyphae and agar, and has a high hyphae density.

At this point, several parameters of mycelium growth are known as incubation time, diameter, change of hue, spore's occurrence and maturation. All these parameters will be important in further analysis to decide a path for this work.

The first proposed methodology, stab culture is presented. After 24 h of incubation, the mycelium has grown as “Day 1” in Table 2, observed with the microscope. It has a high hyphae density, and the centre is a big black spot, which makes impossible the focussing of the image, as is shown in Figure 17. In addition, after 11 h of incubation the mycelium has not grown yet, in some cases even after 12 h. But at 16 h, the mycelium has grown as shown Figure 18, with short hyphae, a massive black spot, low contrast between hyphae and agar, but also with garbage, from the waste that was carried with needle tip. In this way, these results focused the project on looking for a mycelium with no massive black centres, high contrast between hyphae and agar, younger mycelium and no trash.

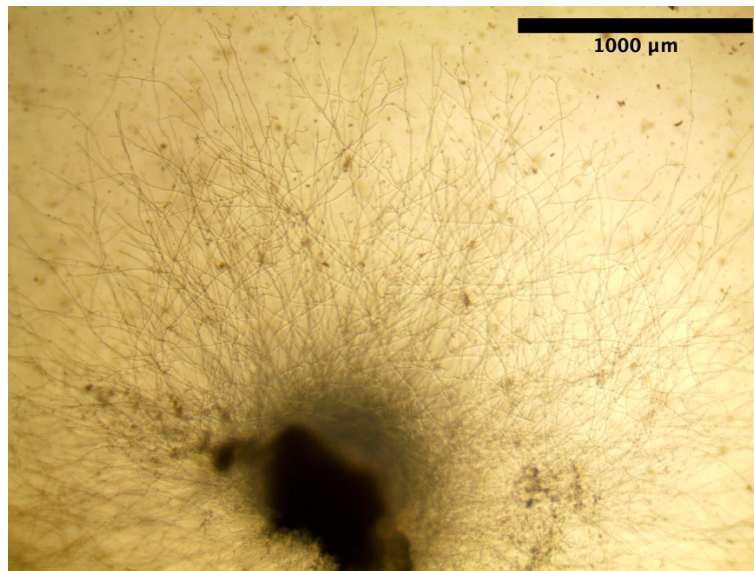


Figure 18. Image of mycelium capture with an 80x lens at 16 h after incubation, it is appreciated the low contrast between hyphae and agar, but at this time the mycelium had not high hyphae density, however, the black spot centre is still here.

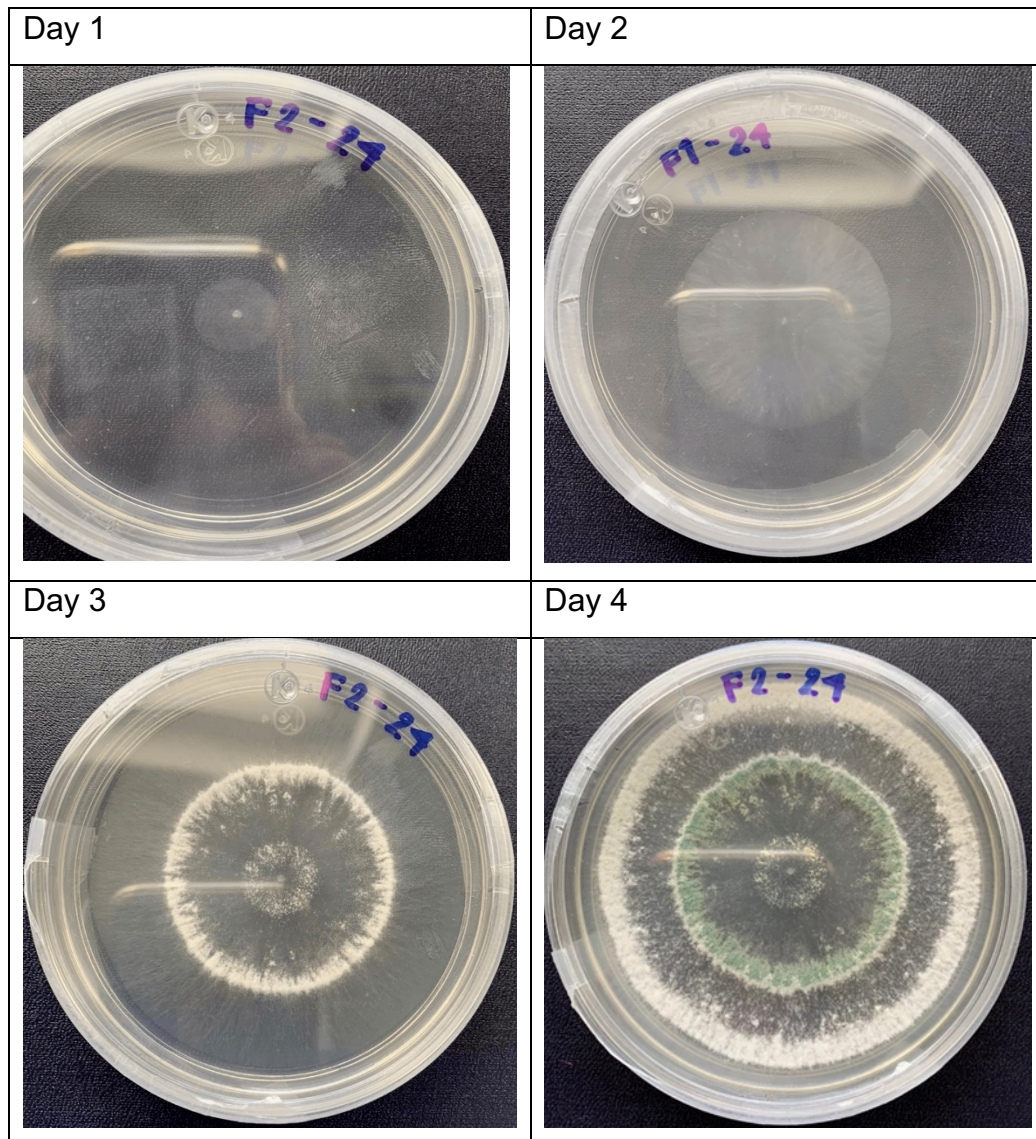


Table 2. Photo-conidiation process. Day 1 has only 24 h of incubation. Day 2 has two cycles of incubation and 1 cycle of exposure, the mycelium is hyaline, no conidiation halos are present. Day 3, after 3 cycles of incubation and 2 of sunlight exposure it can be appreciated two conidiation halos, one of them is whiter than the small one. Day 4, after 4 cycles of incubation and 3 of sunlight exposure, three conidiation halos show up, one of them is green, indicating the maturation of spores.

The second experiment was planned to fulfil the characteristics missing from the first. In this sense, to increase contrast in images, the volume of PDA was reduced to 7 mL per Petri dish ensuring a thin layer of medium (~3 mm of thick). The images taken by optical microscopy revealed a single spore germination, an absence of a massive centre. Also, younger mycelium was obtained, but at 37 h after inoculation. Time variation is produced by the spore's germination time as it takes time to the spore to adapt to the medium. This does not happen with the

previous method, because when collecting spores with the tip of the needle, it carries a cluster of hyphae and spores, where hyphae grow faster than spore germination. (Roncal & Ugalde, 2003). The spore concentration in solution was not measured because in this research is interested in quantifying a single mycelium and not the spores contained in the solutions. However, we collect from experiments the number of germinated spores from solutions 1:50, 1:100 and 1:1000, and they were 25, 12 and 1 spores per Petri dish, respectively. Additionally, the dilution of the cluster on the needle tip, reduces the presence of unwanted material in the mycelium.

At this point, the mycelium has the characteristics required to collect images with high contrast, without garbage and a massive centre, but with a longer incubation time, so the next step was to calculate the spore's germination time.

Spore's germination

With the latest inoculation method, it was tested how much time does spores take to germinate in the medium. This experiment was reviewed every two hours from 24 to 34 h after incubation. It was detected that at 29 h, more than the half of spores have germinated. A fresh solution of a 1:100 ratio was used, where approximately 15 spores in the dish were found. This test was repeated 3 times and in the check-up at 30 h, the spore's germination was higher than half with 11 spores. Otherwise, at 28 h, the germination was below half with only 5 spores germinated. Therefore, approximately at 29 h after incubation the half of total spores were germinated, as shown in Figure 19.

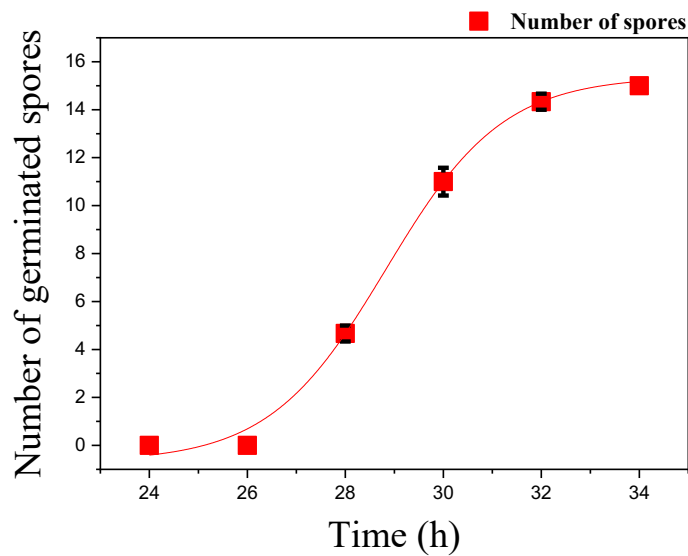


Figure 19. Plot of number of germinated spore's vs time. Each datapoint (red squares) represents the average number of germinated spores through time of incubation with 3 repetitions ($N = 3$). Red line is a sigmoidal fit. With a medium value of 28.8 ± 0.08 h.

Image acquisition and digital processing

The acquisition presented a different difficulty depending on the size of mycelium. The 8 h mycelium required approximately 10 images to fully capture it. Meanwhile, the 11 h fungi were bigger and 40 – 50 images were needed to recreate them. For the biggest mycelium it was captured 70 – 100 images. Thus, the process was methodical, because the focus was varied in every image and images with 200x lens were captured as well.

However, we face two problems, blur and magnification in closer hyphae. In central areas, hyphae were close without touching each other and the pictures taken with 80x lens showed black spots. To fix this problem, it was used a 200x objective lens in these areas to obtain an image without black spots and used further to recreate the mycelium. Against blur, two images were taken with focuses on different parts of the field of view.

Images captured from the first inoculation method were not adequate to this project, due to massive black spot in the centre, low contrast and mycelium was large.

Meanwhile, digital processing consisted in pre-processing, stage described in previous chapter, all images of experiment two were successfully binarized, this refers to the images only have two values, 255 (white) or 0 (black), as shown in Figure 13. Also, images do not present black spots and have the highest contrast between hyphae and the background. However, the hyphae surroundings in some cases presented a few pixels out of place, due to pre-processing stages. To solve this, the brush tool was used once the mosaic was assembled.

Mosaic assembly

The mycelium assembled previously does not have any complication through the process. As was stated before, some images after pre-processing had issues like the union of two close hyphae or places where more than 3 hyphae joined, where the assistance of images captured by the 200x lens was needed to define hyphae. As well as pre-processing, the difficulty increases with the size of mycelium. Young mycelium required 15 minutes to be assembled. Meanwhile, medium and large took 1 – 2 h to be completed. Additionally, the manual smoothing for medium and large mycelium required at least 2 hours to be completed.

Next, three mycelia are presented in Figure 20 - 22, these are 8 h, 11 h and 14 h after germination, respectively. It is notable that size, extension, hyphal density and ramifications change considerably through a few hours.

As was stated in Chapter II, 5 mycelium were cultivated to analyse at 8, 11 and 14 h, then they were analysed, and they are presented in the Annex.

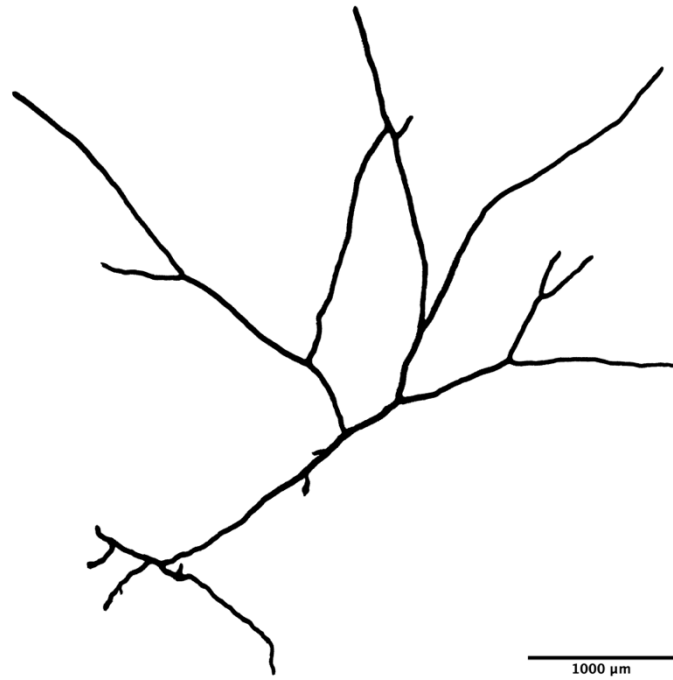


Figure 20. Mycelium completed after mosaic assembly. This mycelium is representative of the sample size captured at 8 h after spore's germination. Approximately 10 images were used to assembled and contains 39 nodes.

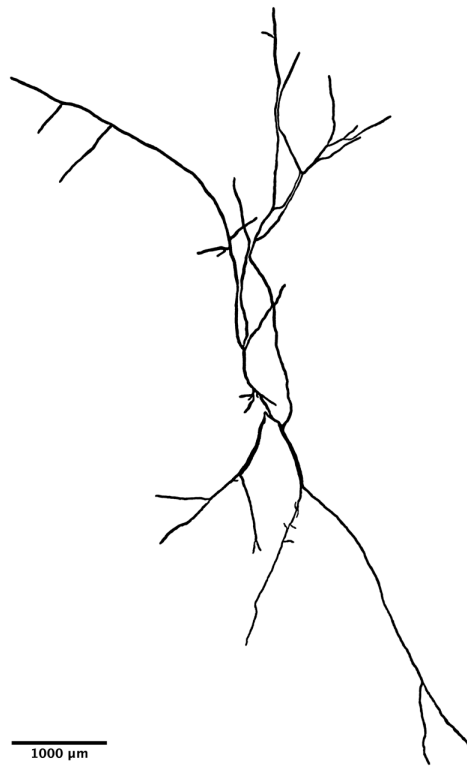


Figure 21. Assembled mycelium of 11 h after spore's germination. Approximately 25 images were used and has 75 nodes. This image has already the correction of black spots and the use of brush tool.

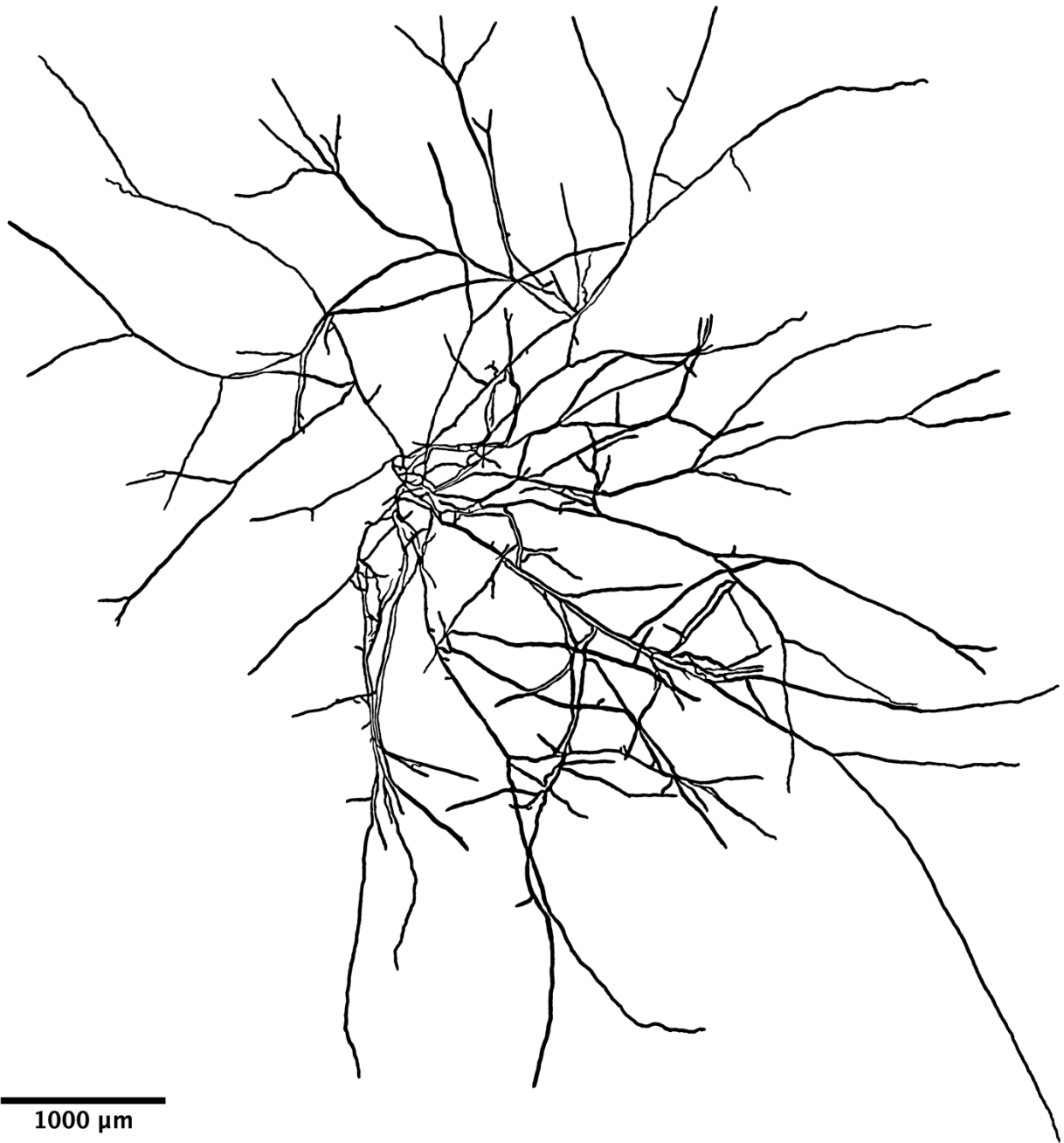


Figure 22. *Mycelium after 14 h of germination, approximately 70 images were used to assembled it. This mycelium has 557 nodes and 133,000 μm of total length.*

Network Extraction

As was stated before, NEFI extracts the network selecting nodes and edges as was explained in Chapter II, nodes are marked as a blue square, meanwhile, edges are drawn like red straight lines, as shown in Figure 23.

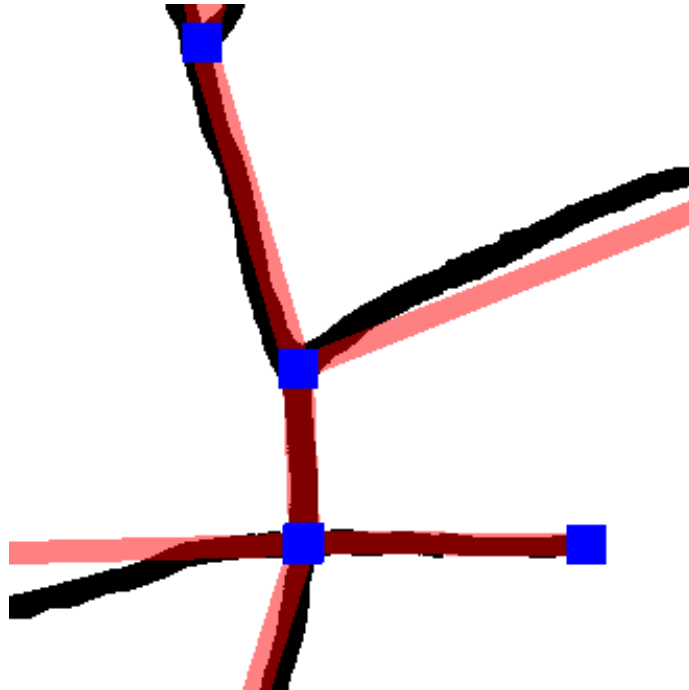


Figure 23. Network extraction by NEFI in a part of mycelium. NEFI marks with blue squares the nodes and edges with straight red lines.

Also, NEFI can detect the degree of the selected nodes, it assigns values like 1, 3, 4, 5, or higher depending on the number of connections, as shown Figure 24. The software recognizes the hyphal tips as nodes of degree 1, circled in blue. On the other hand, the branching hyphae are recognized as nodes of degree 3, marked with red circles. Then, nodes of degree 4 are crosses between two hyphae, circled in pink. Additionally, nodes with higher degree were a problem from NEFI to be detected, due to thinning process.

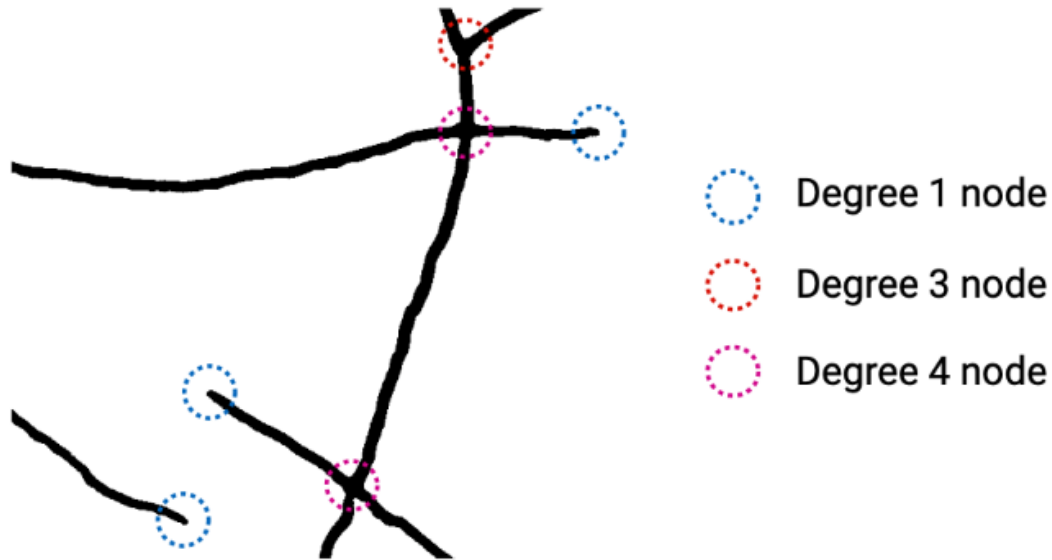


Figure 24. Section of a mycelium indicating the degrees of the nodes. Blue circles indicate nodes with degree 1. Red circles indicate nodes with degree 3. Pink circles indicate nodes with degree 4.

Apparently, NEFI works well, but there were some challenges before obtaining the results we wanted. Some of these challenges were image format, size image, the pipeline, segmentation process and data. Fortunately, all these challenges were overcome. The image format was converted into a “.tiff” format and the size of the images were around 4500 x 3800 pixels, therefore, NEFI took a minute or even more to process the mycelium.

On the other hand, the pipeline structuration was tested several times, specifically in “segmentation” category, because when using an algorithm other than described in Chapter II caused several node detections errors to appear. The image process NEFI does is through thinning the mycelium. In this way, various errors appeared because in the crosses where 4 or more hyphae intersected, the thinning process deviated the hyphae, marking two nodes of different degree instead a single node of degree 4. This problem was solved editing the crosses on ImageJ, as is showed in Figure 25. Finally, the data obtained includes a list with coordinates, length, width and node degree. From this list the data used was length, nodes degree and coordinates, width was not used due to pre-processing and mosaic assembly

change the original values for hyphae, also, it is irrelevant due to hyphae have on average the same value.

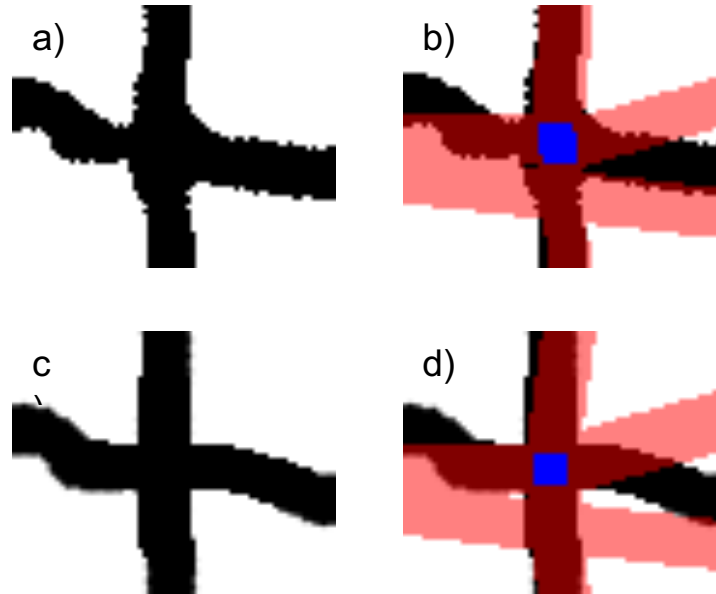
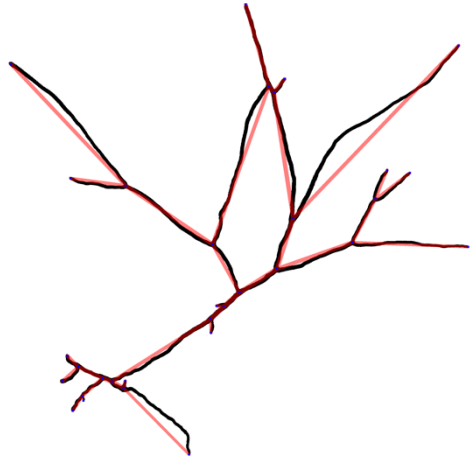


Figure 25. Exemplification of the edition of nodes with degree 4. Image (a) is the image after pre-processing. Image (b) is the previous image after NEFI extraction, but with two very close squares instead of one. Image (c) is the image (a) with the cross edited. Image (d) is the extracted network with the cross edited, as we can see this only has 1 blue square, which means only one node is recognized.

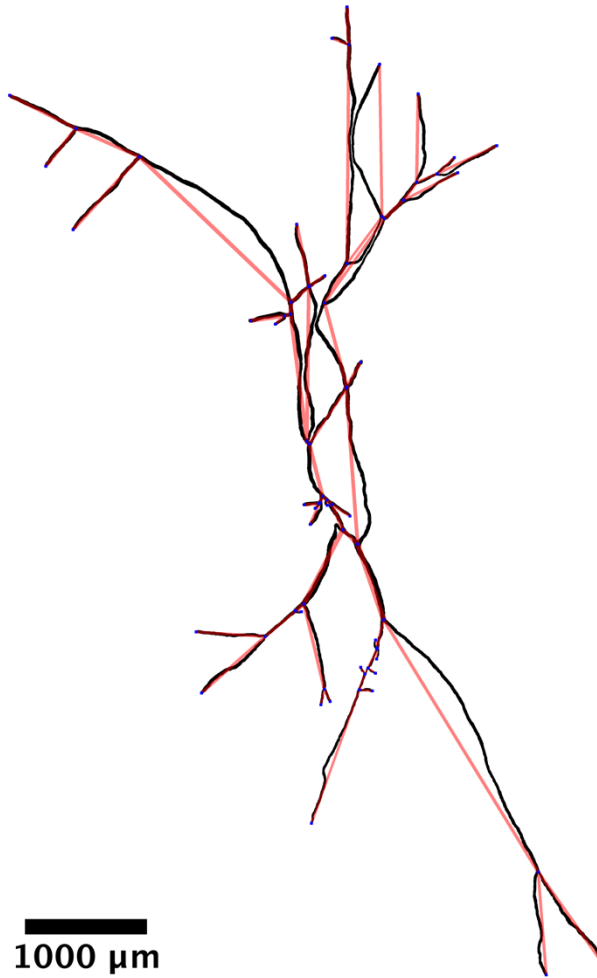
The data was filtered by coordinates, where two formats were distinguished. The first, was the coordinate with the format (y, x) and a number, apparently associated with the node degree. The second format was the coordinate with the same format and a set of parameters associated with edges. These parameters were length in pixels and width. After applying the conditional rule described in Chapter II, the degree nodes and lengths were accounted to obtain the number of nodes, their degrees, number of edges, total length of mycelium and the average length.

The images of Figure 26 – 28 are mycelia after network extracting process, each mycelium correspond to 8 h, 11 h and 14 h, respectively. The rest of mycelia are in the Annex. In addition, lengths were converted from pixels to micrometres using the conversion described in previous chapter. Then statistical analysis was carried out and is presented below.



1000 μm

Figure 26. Mycelium of Figure 20 after network extraction. Red lines are edges, blue squares are nodes. This mycelium is representative for 8 h set.



1000 μm

Figure 27. Mycelium of Figure 21 after network extraction. Red lines are edges and blue squares are nodes. This mycelium is representative for 11 h set.

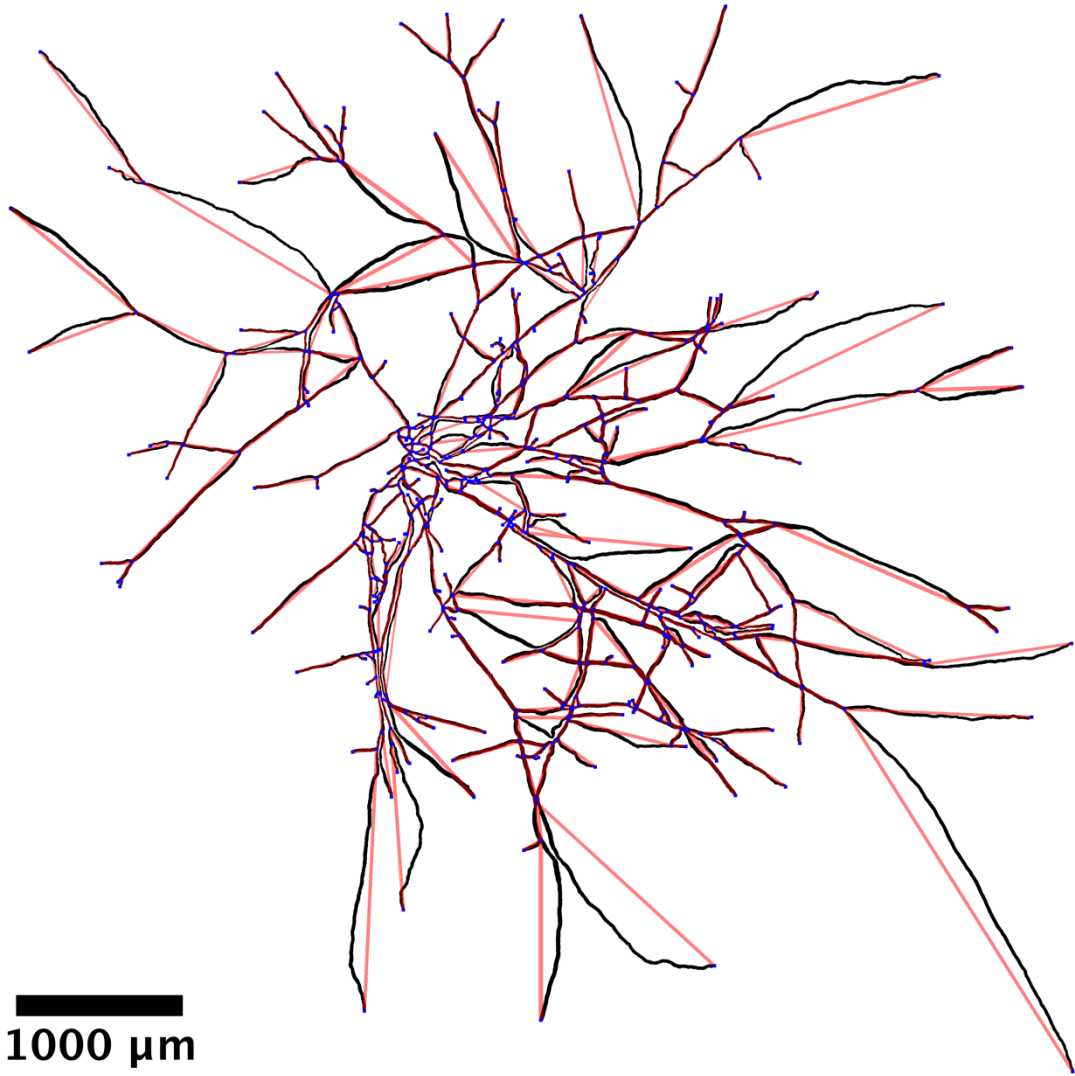


Figure 28. Mycelium of Figure 22 after network extraction, representative for 14 h set. Red lines are edges and blue squares are nodes.

Statistical analysis

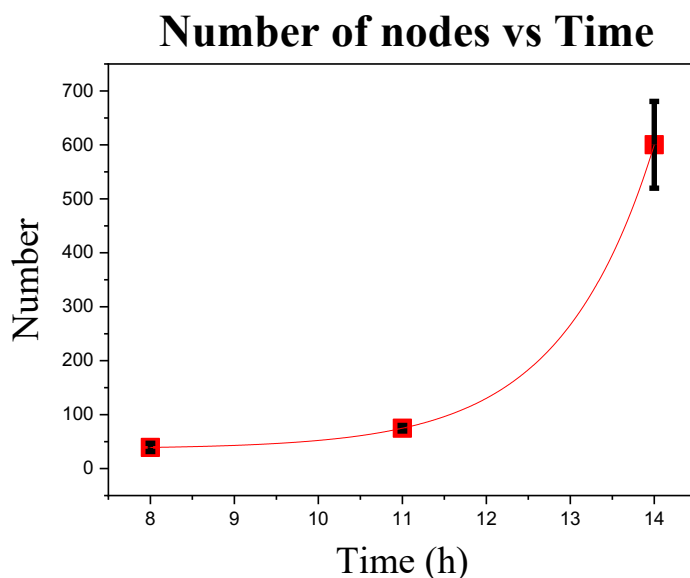


Figure 29. Graph of node number vs time (after germination). Each datapoint (red squares) represents the average of $N = 5$ repetitions. Error bars: standard error of the mean. Red lines are an exponential fit to data. With a value of $t_1 = 1.114 \pm 2.25E-16$ h. Where t_1 is the denominator of the exponential function usually called τ .

As we can see, Figure 29 represents the total number of nodes in mycelium at 8, 11 and 14 hours after the spore's germination. It is appreciable that after 8 hours of growth one mycelium has less than 50 nodes. After 11 hours the mycelia have less than 100 nodes, but at 14 hours it has approximately 600 nodes. This plot shows an exponential growth in the appearance of nodes, it is explained by the augmentation of ramifications in the centre of mycelium through time.

As we can see, in Figure 20, the centre of mycelium at 8 h is barely distinguishable, hyphae are long and has a few ramifications. Then, at 11 h, mycelium has more ramifications and increase their total length. Finally, at 14 h after germination, the mycelium centre is distinguishable and has a high number of ramifications. This happens because mycelia want to take advantage of all the nutrients in its neighbourhood and connect nearby hyphae as consequence. This process is reflected in the number of nodes of degree 1, 3 and 4; it is reflected in Figure 30.

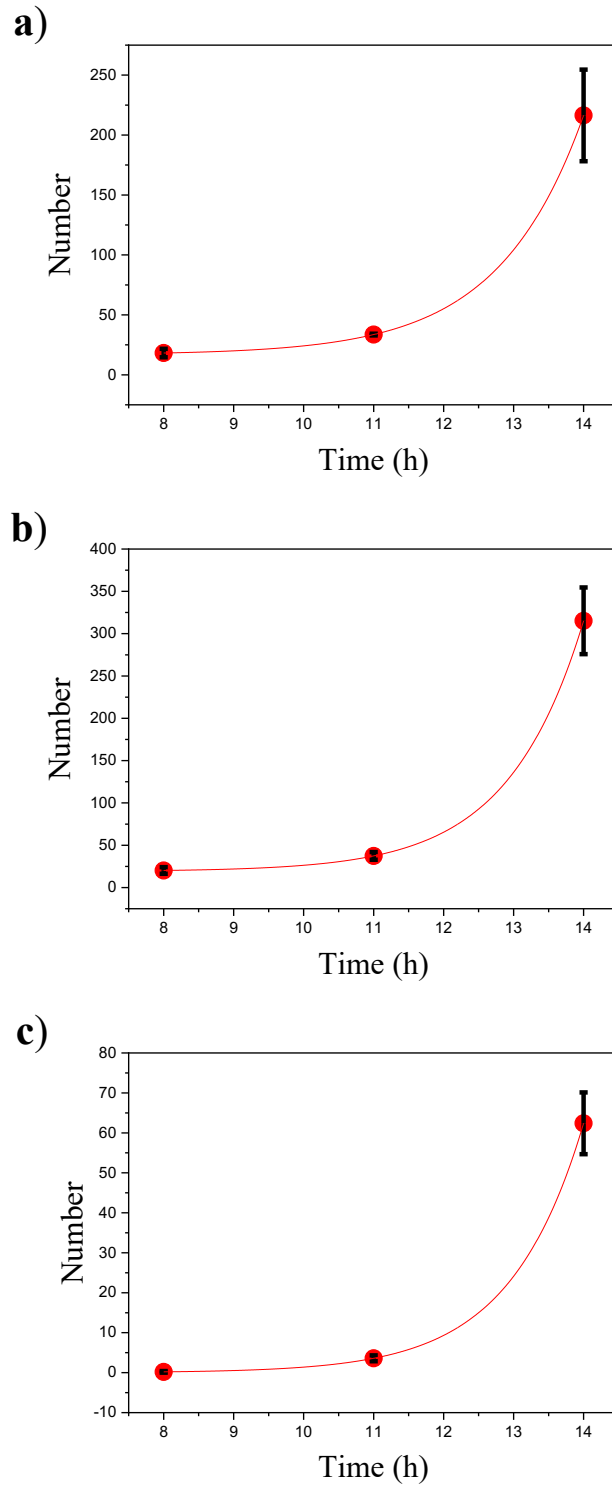


Figure 30. Node degree number at different times after germination. (a) are nodes of degree 1 through the set of times. (b) number of nodes with degree 3 and it increase in time. (c) number of nodes with degree 4 through time. Each datapoint (red circles) are the average of the number of nodes presented in 5 mycelium per time. The bars are the standard error calculated. Red lines are an exponential fit to data. With the following values of τ : $1.212 \pm 2.84E-16$ h, $1.078 \pm 2.49E-16$ h and $1.052 \pm 4.81E-16$ h, respectively.

As it can be appreciated, number of nodes with different degrees that were measured have an exponential behaviour, derived from the augmentation of ramifications explained before. For nodes of degree 1 at 8 h the number of nodes were 18, after 3 h the number rises to 34 nodes and 6 h after the number rises to 216 nodes. Nodes of degree 3 started with 20 nodes at 8 h, 37 nodes at 11 h and 315 nodes at the last time. Finally, nodes of degree 4 started with 0 at 8 h, but increased to 4 nodes at 11 h and 62 nodes at 14 h. The values reported previously represent the average of 5 repetitions ($N = 5$) per time.

In addition, the analysis of degree nodes higher than 4 was not carried out because they did not appear until 14-hour of germination. For younger mycelium (8 and 11 h) degrees higher than 4 did not appear because of the level of branching. The higher degree nodes appear since 14 h and these could be of degree 5, 6 or even 7, but only one or two were presented per mycelium.

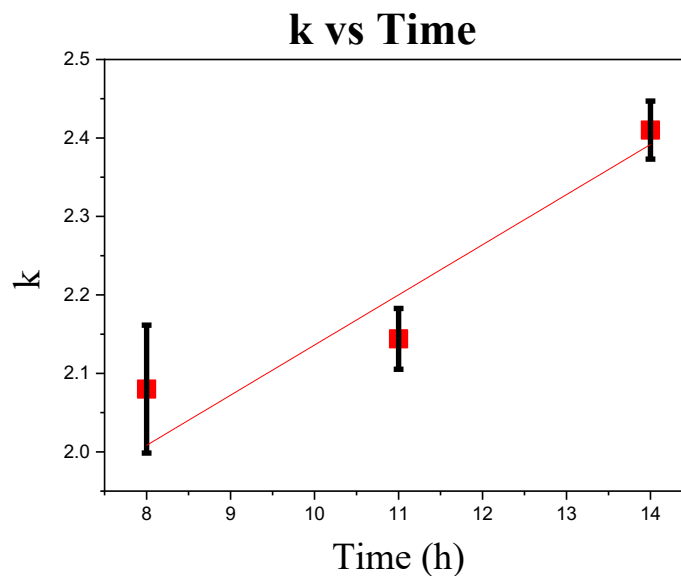


Figure 31. Average node degree of mycelium vs time (after germination). Each datapoint (red squares) represent the average node degree of 5 mycelia per time ($N = 5$). Error bar: standard error calculated to the mean. Red line is a linear fit to data with an R -square = 0.90, with a slope = 0.067 ± 0.02 .

On Figure 31, is presented the plot of “k” value versus time. This parameter is the average node degree of the mycelium. It can be observed that k values increase with time. Started with 2.08 at 8 h, then 2.14 for 11 h and 2.4 at 14 h. The k value also means that if we choose a random node, it has the probability to have two edges connected to it. However, in this network, nodes with degree two are not possible, because it is a single node with only two connections. This structure does not show up in this network because the mycelium branches, creating three hyphae, as shown in Figure 24.

As was stated before, the k value is the average node degree of the mycelium. This value increases due to the augmentation in the number of nodes with degree 3, 4 or higher in the mycelium through time. Therefore, this value represents the augmentation of the complexity of the system in the first 14 hours of growth.

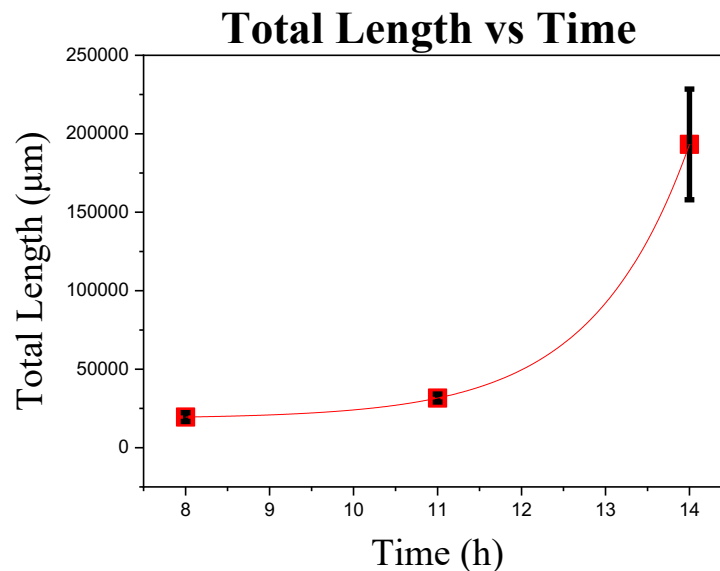


Figure 32. Mycelium length vs time (after germination). Each datapoint (red squares) is the average length of 5 mycelium per time ($N = 5$). Red line is an exponential fit to data, with a value of $\tau = 1.15 \pm 3.53E-16$ h. Error bar: standard error of the mean.

The Figure 32 shows the total length of mycelium at 8, 11 and 14 h, which are 19,517 µm, 31,615 µm and 193,234 µm, respectively. These are the average values

obtained with 5 repetitions ($N = 5$) per hour. Also, this plot has an exponential growth, supported by the mycelium growth, where hyphae are longer due to branching and the apical growth of the external hyphae. Additionally, hyphae density increases in the centre of mycelium, and this could be represented in Figure 33.

The average length of mycelium at the previous described times are $518 \mu\text{m}$, $378 \mu\text{m}$ and $237 \mu\text{m}$ respectively. This length has the particularity to decrease with the passage of time, due to hyphae made new connections via anastomosis with sub-apical growth. The creations of new connections in the centre of mycelium increase the number of nodes and their degrees, total length and decreasing the length in hyphae between nodes. Therefore, it is expected that older mycelium has a higher hyphae density with nodes with a higher degree than those analysed in this project.

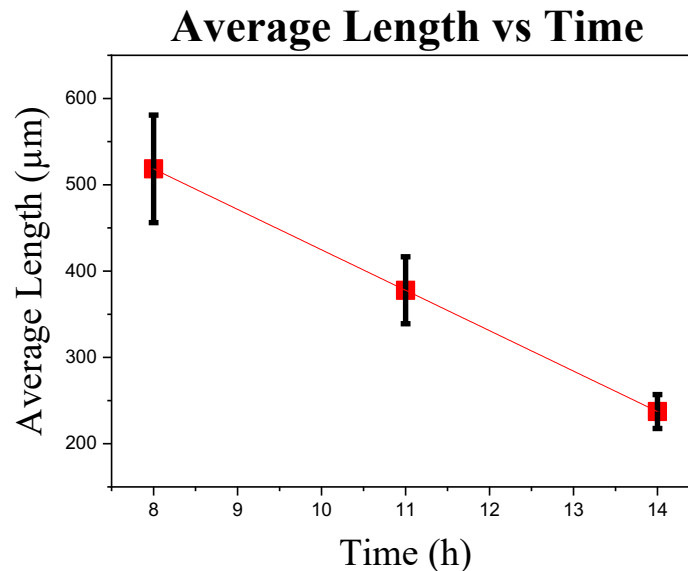


Figure 33. Graph of the average edge length vs time (after germination). Each datapoint (red squares) represents the average length of 5 mycelium ($N = 5$) per time. Error bar: standard error of the mean. Red line is a linear fit to data, with a R-square of 1, with a slope = -46.84 ± 0.01 .

G – Hyphal growth unit

In Chapter II, some expectations about this plot have been mentioned. Figure 34 shows the behaviour of growth rate, which it is not constant in the studied time. However, the datapoint at 8 h has a G value over 1000 micrometres, at 11 h the value is 940 and for 14 h is 892. The mycelium growth for *Trichoderma reesei* has a similar plot accordingly with Lejeune and Lecault. (Lecault et al., 2007; Lejeune & Baron, 1997). Where their plots start with a high value of G and then decreases. However, both Lejeune and Lecault, studied the morphological types of fungi during a fermentation process through several hours.

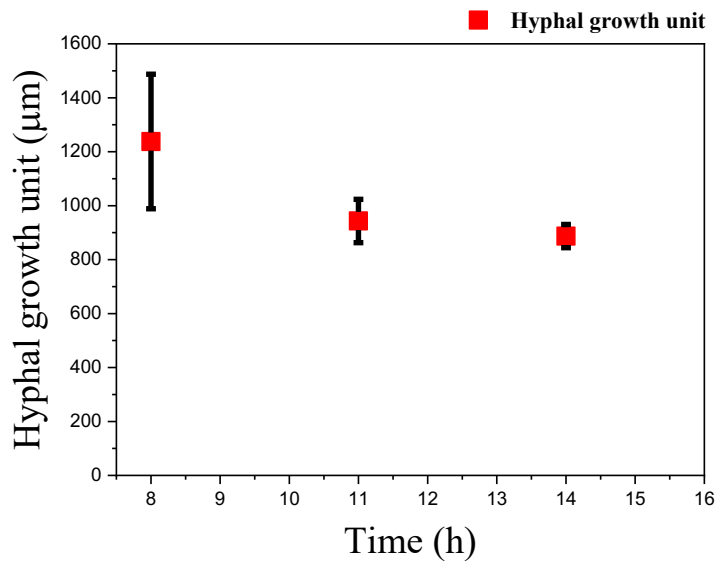


Figure 34. Plot of G vs time. Each datapoint (red squares) were calculated with Equation 4. The total lengths used were the average of 5 repetitions (N = 5). The growth rate it is not the same at the three times.

After 8 h of growth, the mycelium decreases its growth rate. This can be explained by the increase in branching in the centre of the mycelium promoted by the nutrient's concentration gradient. These will move toward the centre of the mycelium as it feeds, leaving the outer areas of the Petri dish without nutrients, promoting a slowdown in mycelial growth, resulting in the formation of hyphal tips (Finn, 1959). This idea could be supported with Figure 35, where, at 8 h, the

difference between nodes of degree 1 and 3 were small. But the difference between them at 11 and 14 h increase, specially at 14 h.

As was stated before on Figure 24, mycelia network has nodes of degrees 1, 3 to 7, these nodes change in time due to mycelium maturation. At 8 hours, the network has less than 50 nodes, which are degree 1 and 3. Meanwhile, three hours after, the number of nodes increase to almost 100, with a few nodes of degree 4. But, at 14 hours after germination, the network has over 600 nodes, with higher degrees. Through maturation process, the mycelium grows trying to explore its environment, then consume the nutrients near of them, creating more branches and increasing its size.

Also, the ramifications changes through time in length and number. It is convenient to remember that the hyphae of *Trichoderma atroviride* is septate. This structure is constituted by fungi cells with no centre, conforming a tube. The main purpose is transport nucleus and organelles inside of it and carry-on nutrients to the Spitzenkörper and make longer the hyphae. However, but the hyphae can be disassembled to restructure the hyphae when nutrients are limited in the surrounding areas.

With these arguments, one may say that hyphae are bidirectional, in other words, the flow can travel in both directions. On the other hand, nodes in the mycelium have the same properties, all of them can share nutrients and chemical signs in a bidirectional flow. Also, the nodes with higher degree and their relevance in the network were not analysed, but a speculation is formulated, these nodes are more important because they have more connection and the shortest path to reach a specific zone could be through them. However, if we analyse the bidirectional flow and the characteristics of nodes into complex networks, then we have a network with the equal nodes and edges with the same property, a undirected network (M. E. J. Newman, 2003), which make it a network with the ability of having a faster reaction speed, but, another analysis must be done to complement this last supposition (Boccaletti et al., 2006).

Also, the k value shows how the network becomes more complex in time, supported by the decreasing behaviour of the average lengths, which is produced by ramifications. Figure 32 shows the evolution of the number of nodes with degree 1 (red), 3 (blue) and 4 (green) through the set of time established before appreciating an exponential behaviour, supporting the increase explained in Figure 30. On the other hand, G values show that the growth of mycelia are not constant, the lengths increase in a faster way than the creation of hyphal tips, which supports the idea of a system which becomes complex in the centre of the mycelium due to the move towards of nutrients.

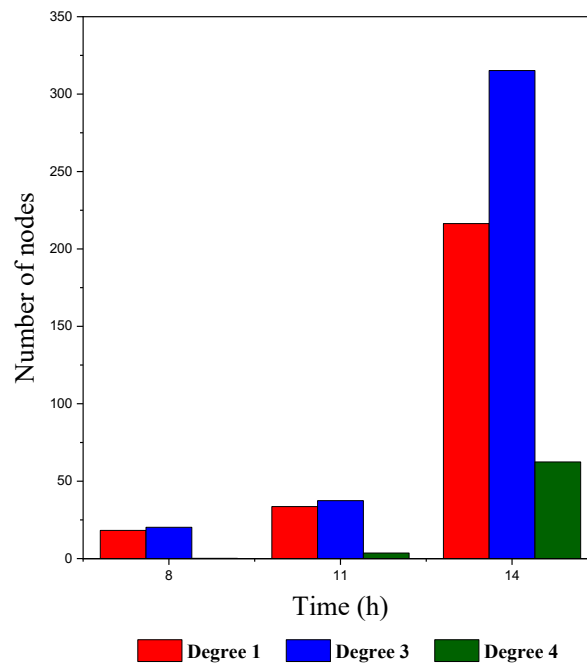


Figure 35. Plot of number of nodes 1, 3 and 4 vs time (after germination). Red bars represent the number of nodes of degree 1 in the three times. Blue bars represent the number of nodes of degree 3 through time. Green bars represent the number of nodes of degree 4 in three times. The reported values are the average of 5 mycelium.

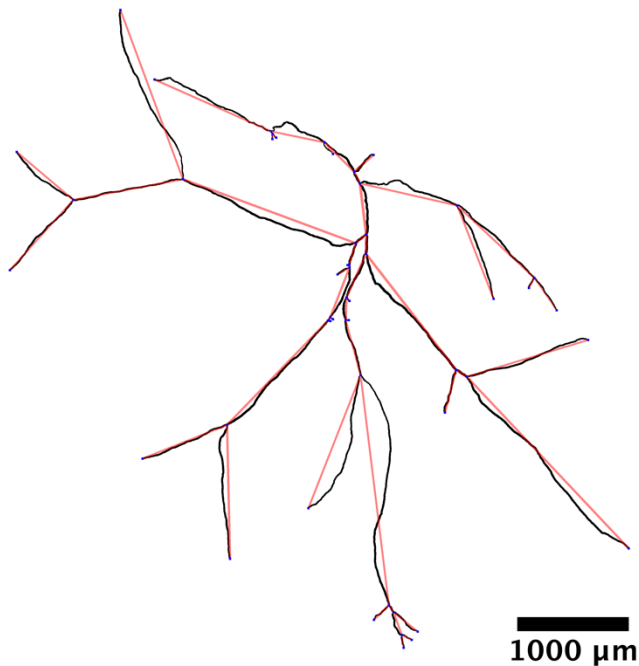
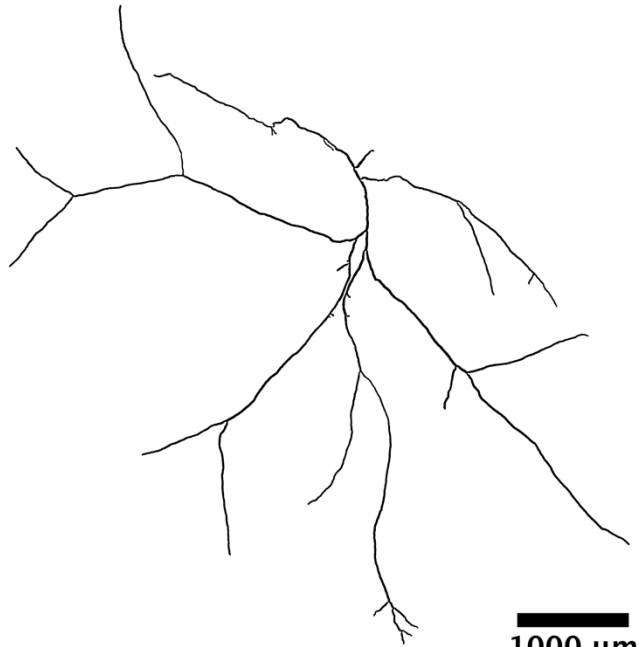
Conclusions and Perspectives

In conclusion, some complex network parameters were extracted from the mycelium fungi of *Trichoderma atroviride*. Also, a methodology for the growth of a single mycelium were developed. Then, it was proposed the pre-processing and the mosaic assemble with two different software's. Therefore, NEFI extracted the data from the mycelium from pictures captured by 80x lens, where edges and nodes are marked properly. The information obtained from NEFI were lengths, coordinates, nodes and the degree of nodes. After analysing the data, we can infer that the mycelium has an exponential growth supported by the increase in nodes, total length, and the appearance of higher degree nodes. On the other hand, through time the network become more complex, as the k value indicates and G value supposed, where the ramification is involved, due to a displacement of nutrients by a concentration gradient. Furthermore, the hyphae have the property of being a bidirectional pathway, making the mycelium a cyclic directional graph and their average length decrease linearly meaning that edges are shortest, increasing the number of geodesic paths and the reaction speed. Therefore, according to Boccaletti, this network has a small world property, however, the growth and aging process is a dominant characteristic of this network; thus this network is named an "evolving scale-free network", where growth is essential and sites with high degrees acquire edges at higher rates than low degree nodes, we can see this behaviour in Figure 35, where nodes of degree 3 increase the number in a higher way than nodes of degree 1 or 4.

As a way to continue, further analysis must evaluate the properties with a longer time after spore germination. Also, with longer times, some properties as geodesic path, clustering and G could be associated with more complex network, in order to be comparable with other networks. Nevertheless, the extraction of complex networks could be a problem, because in this work NEFI ran images with a high pixel resolution that was at the working limit. Another analysis to be done is to check that this network has a bidirectional graph characteristic in information transferences.

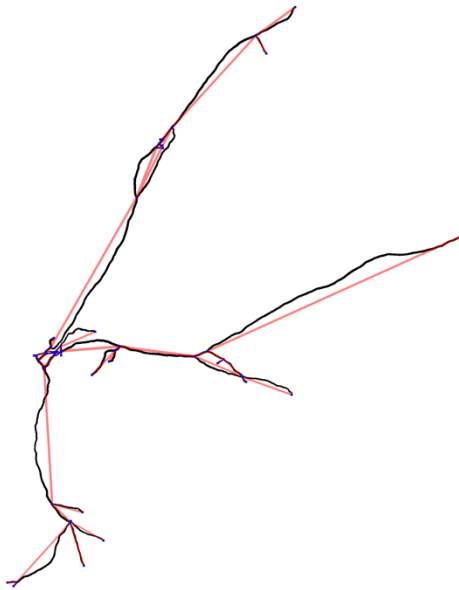
Annex

The following images are incubated for 8 h after spore incubation with the conditions established in Chapter II. A pair of images are showed, the first image is the mycelium after mosaic assembly, the second image is the mycelium after network extraction (red lines are edges and blue squares are nodes).

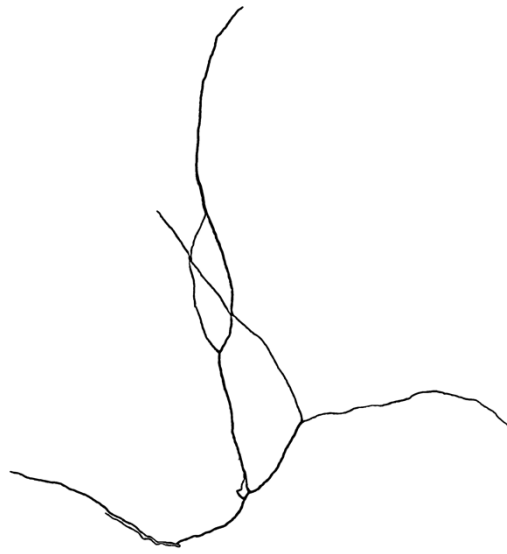




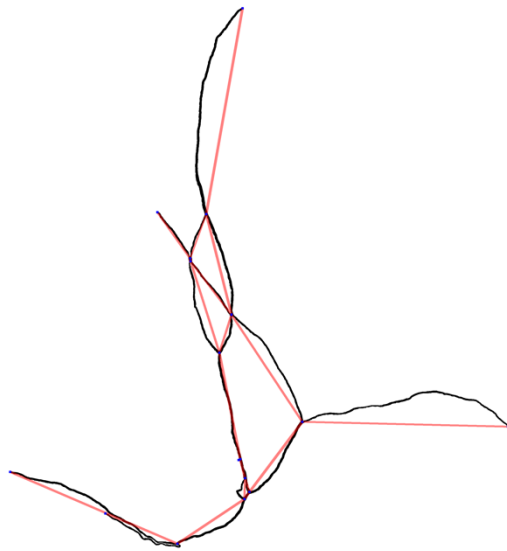
1000 μm



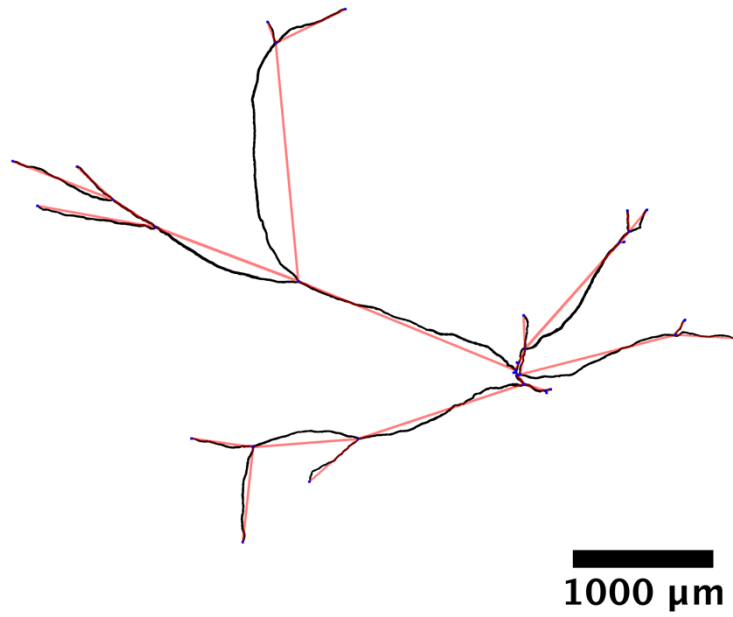
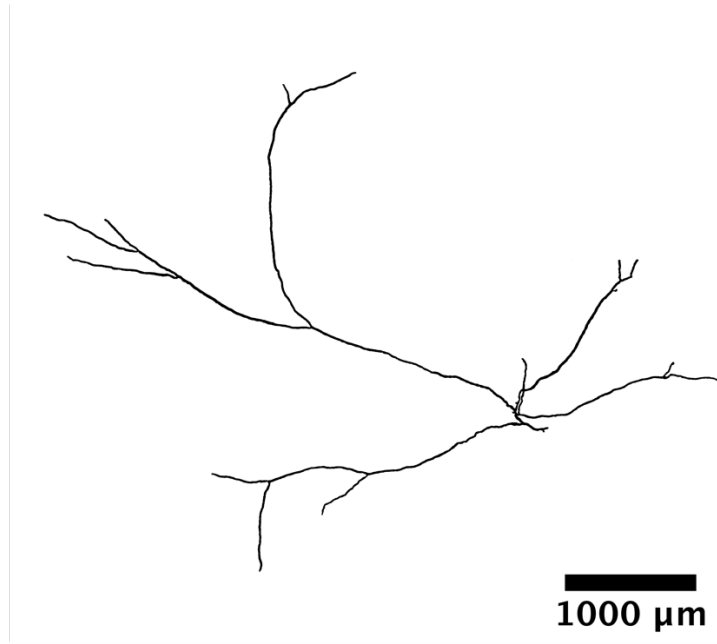
1000 μm



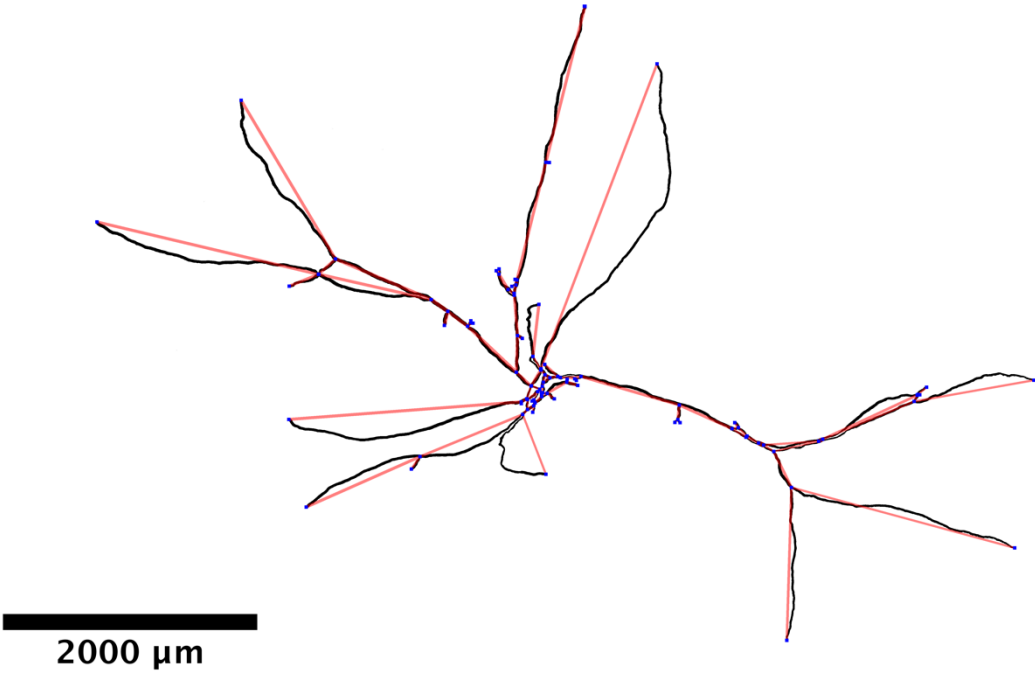
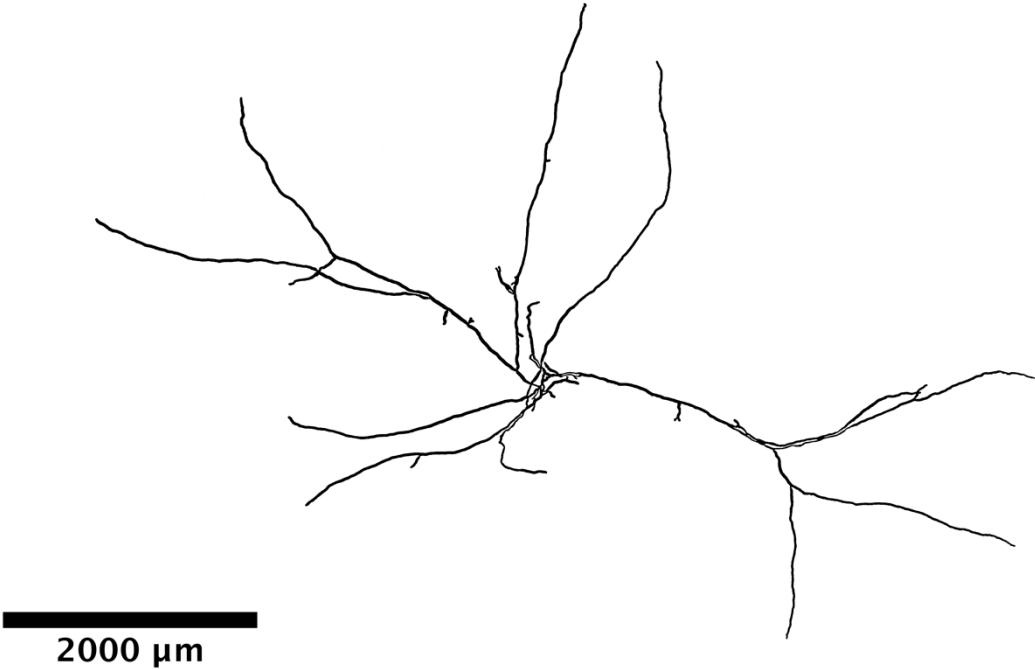
1000 μm

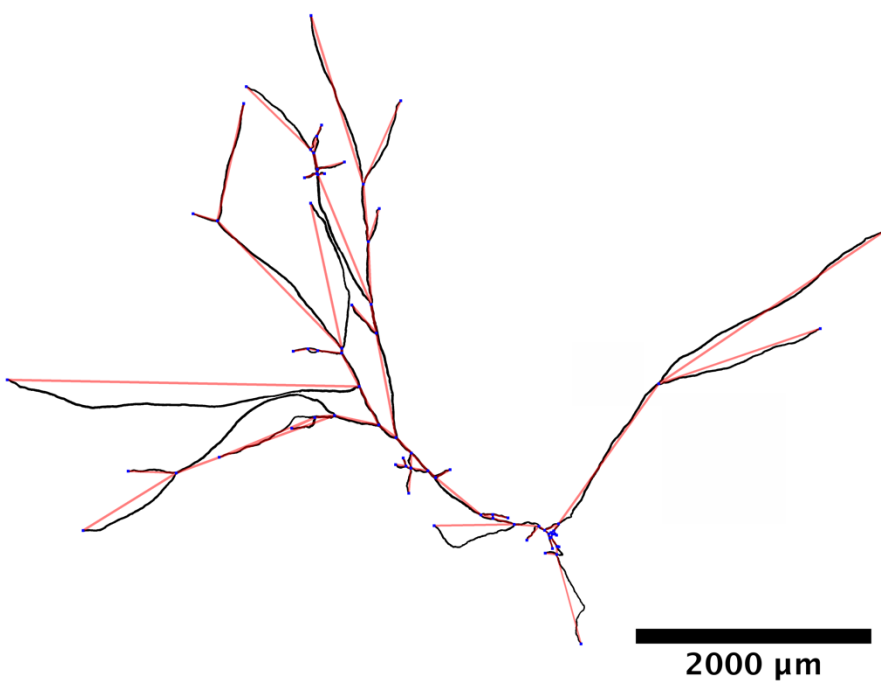
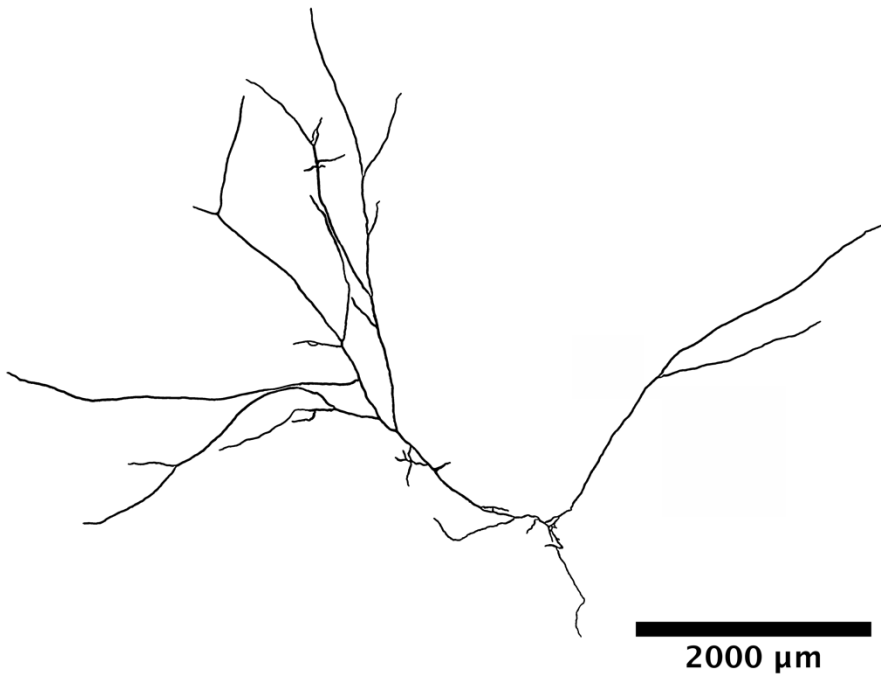


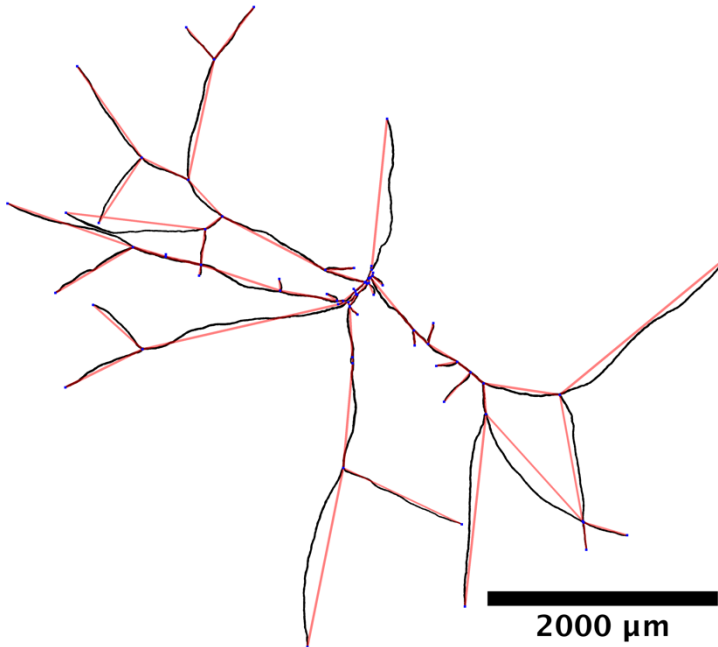
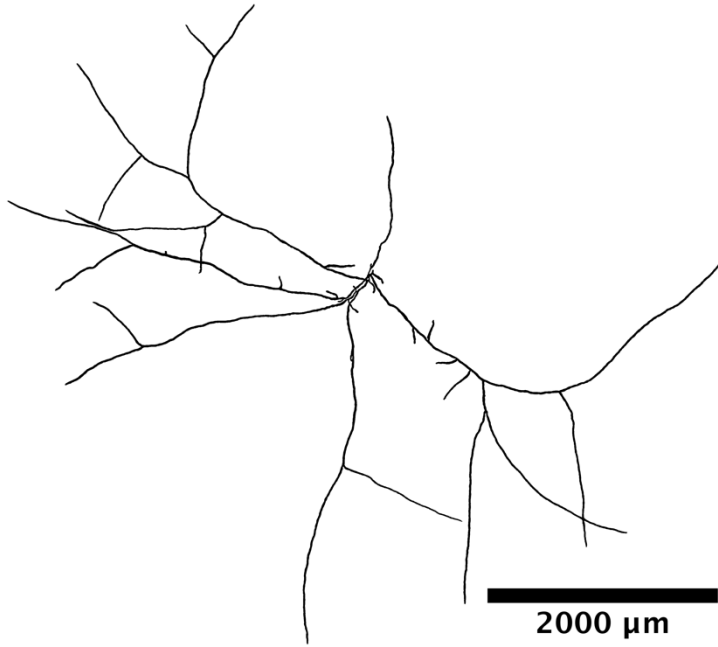
1000 μm



The images presented below are the mycelium and their network extraction after 11 h of spore germination. The conditions of the experiment are described in Chapter II. The first image is the result of mosaic assembly, and the second image is after network extraction (red lines are edges and blue squares are nodes).







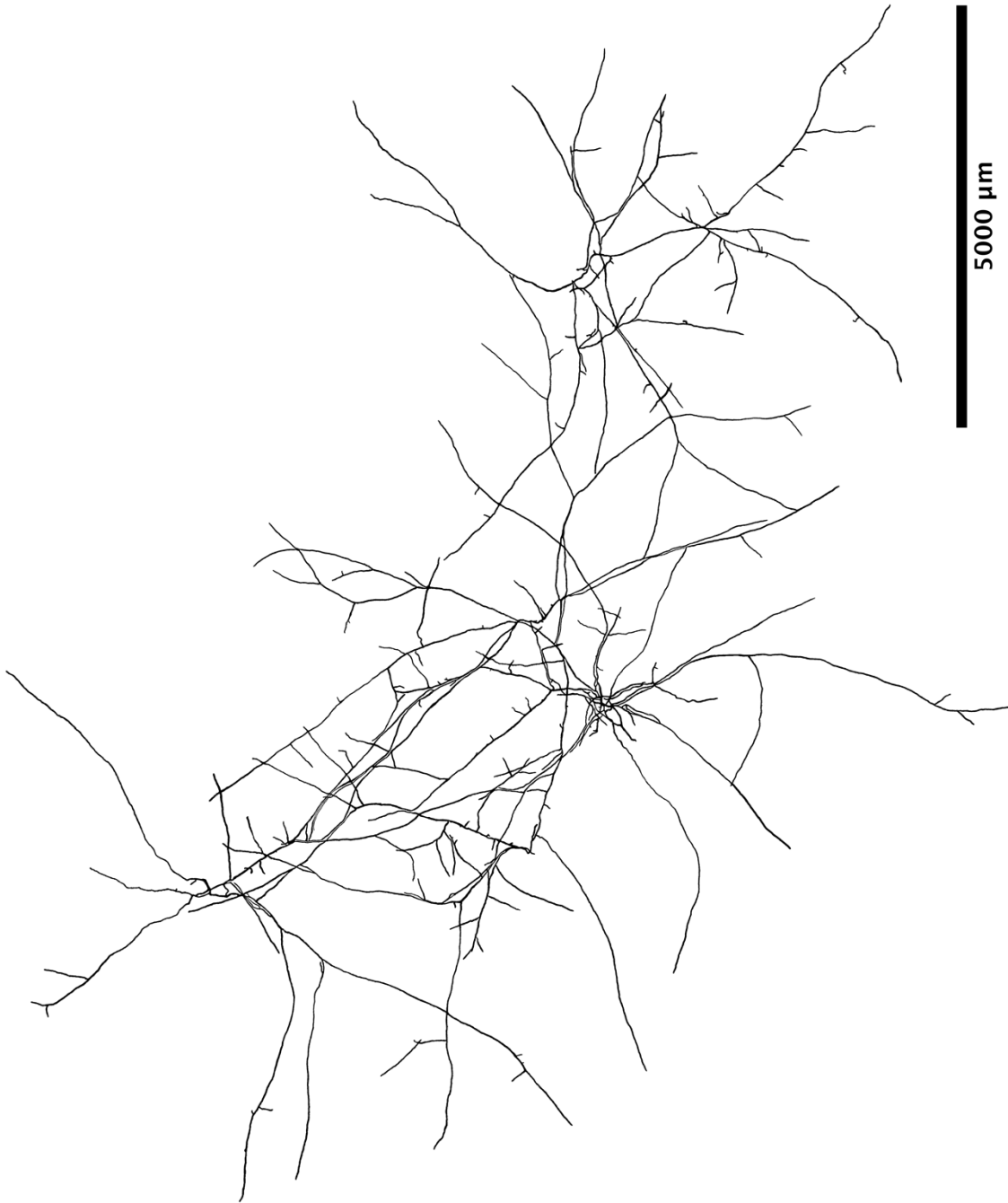


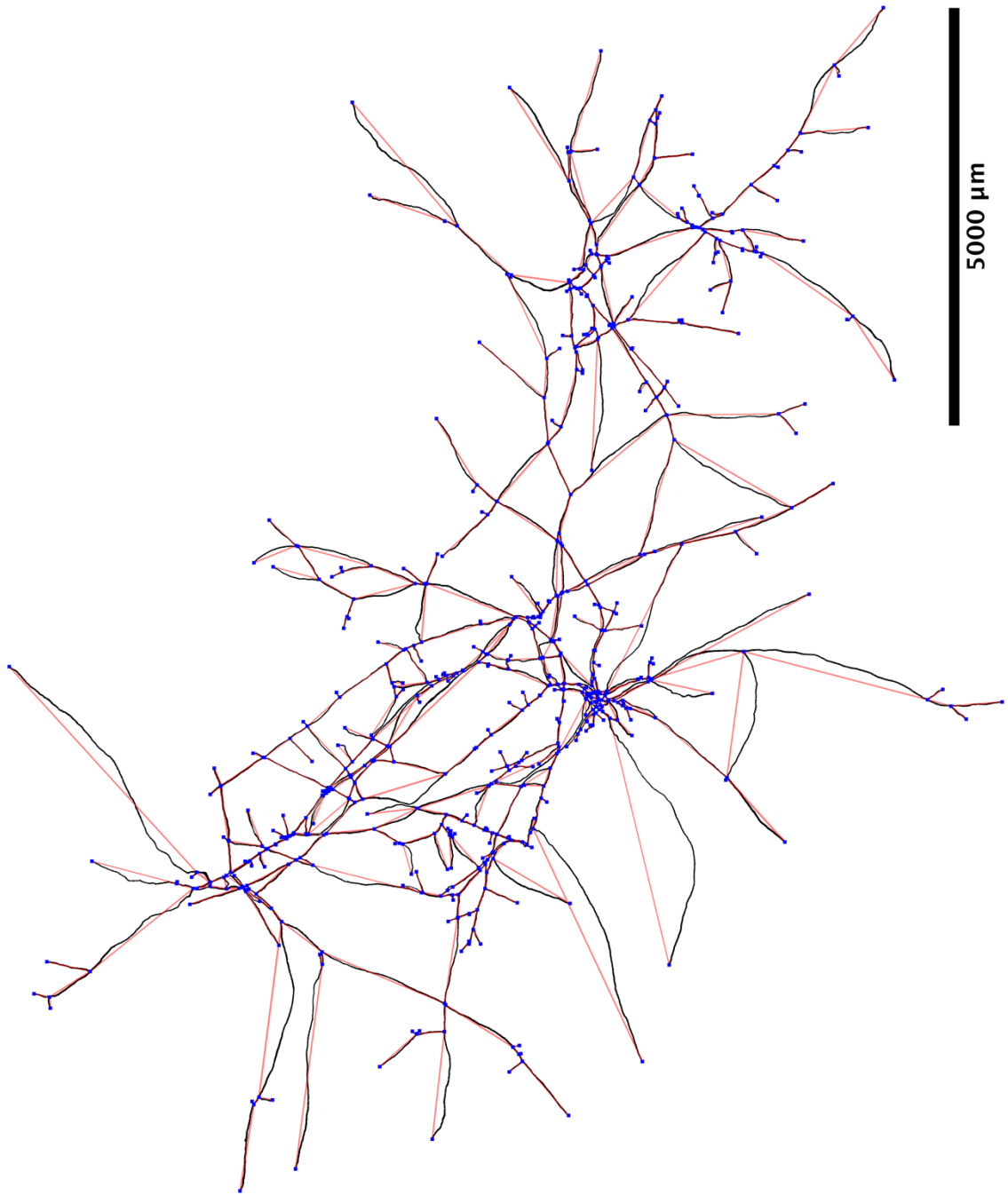
2000 μm



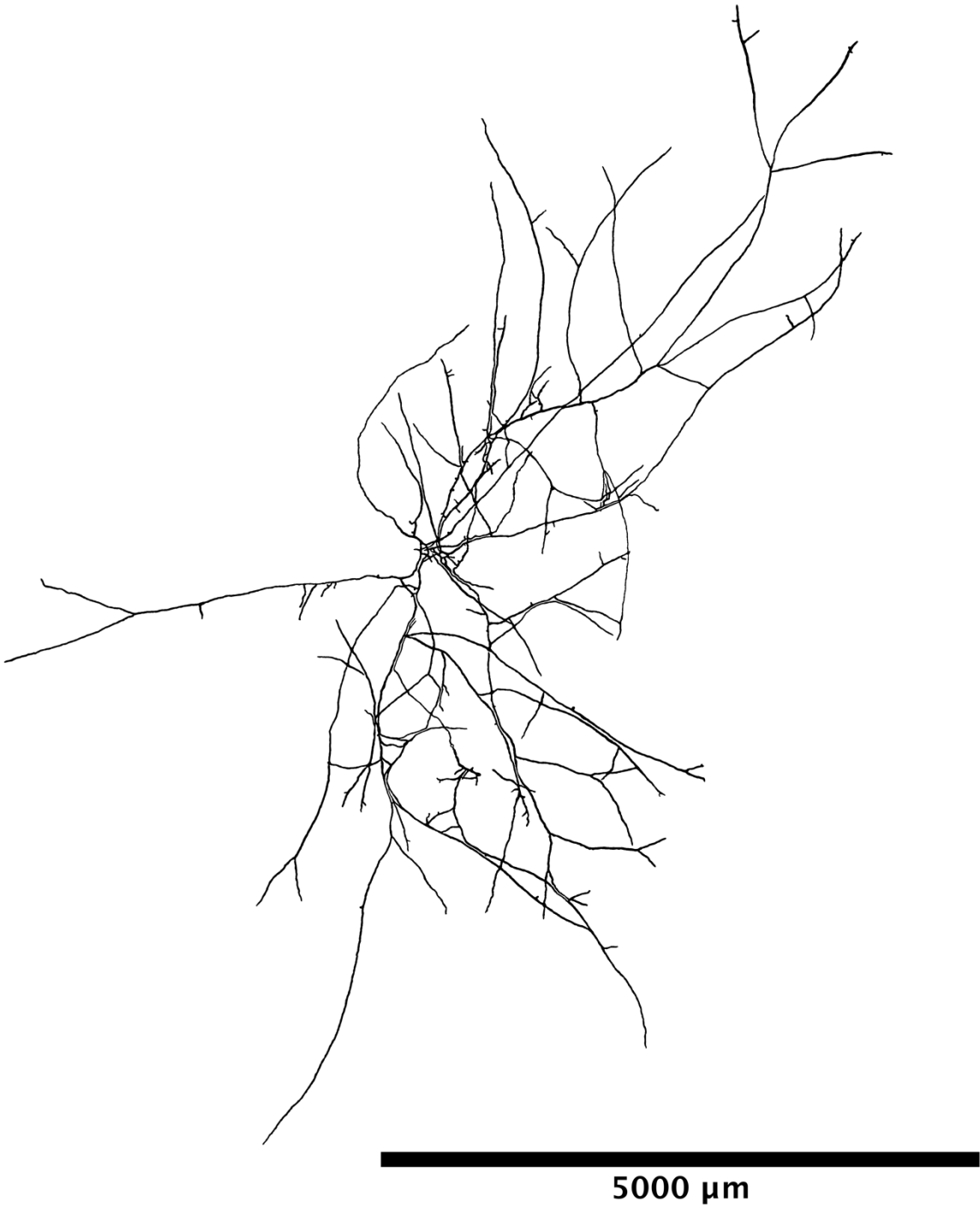
2000 μm

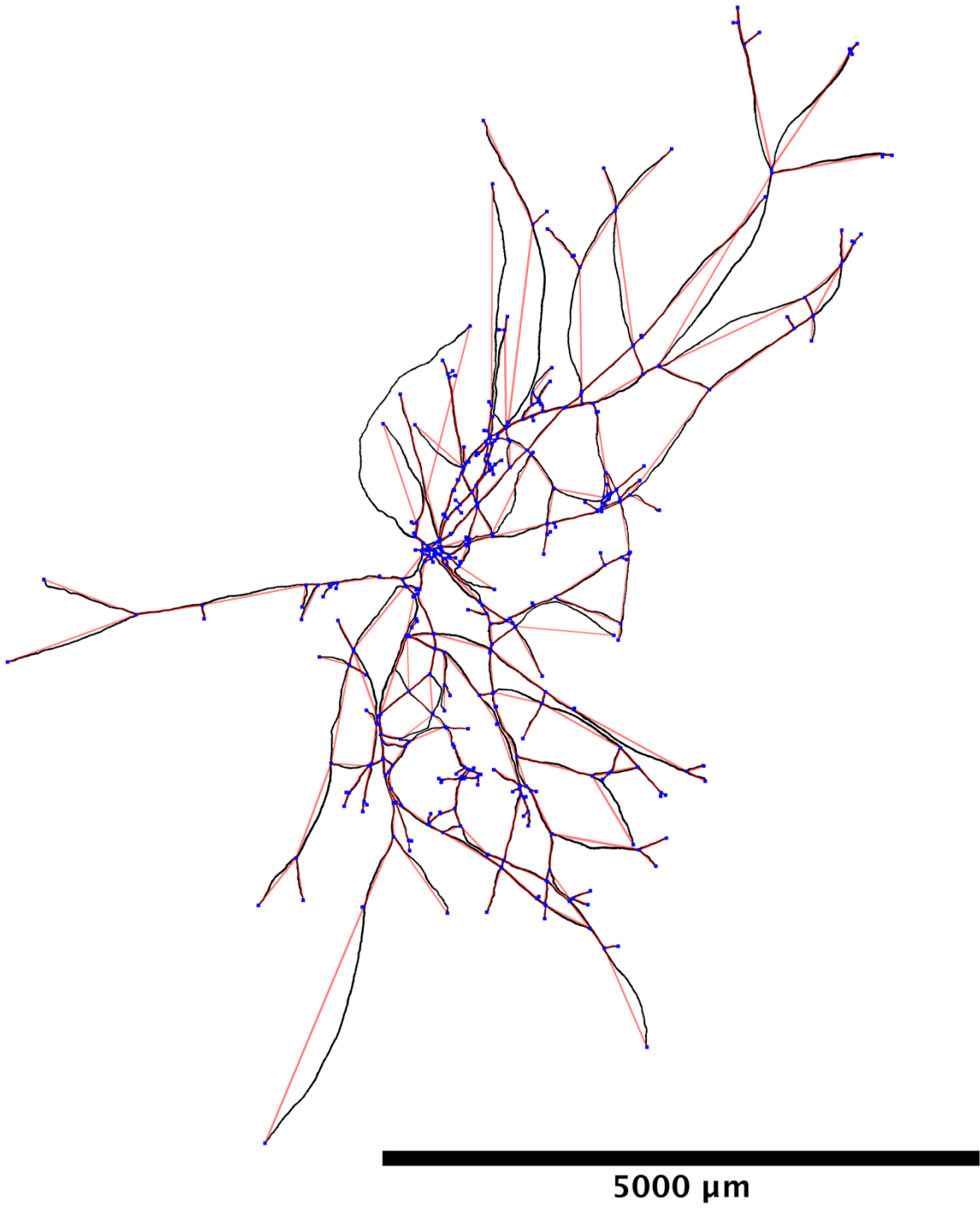
Finally, the following images are the result of mosaic assembly and network extraction (red lines are edges and blue squares are nodes), respectively. These mycelia were incubated for 14 h after spore germination. The conditions are described in Chapter II.

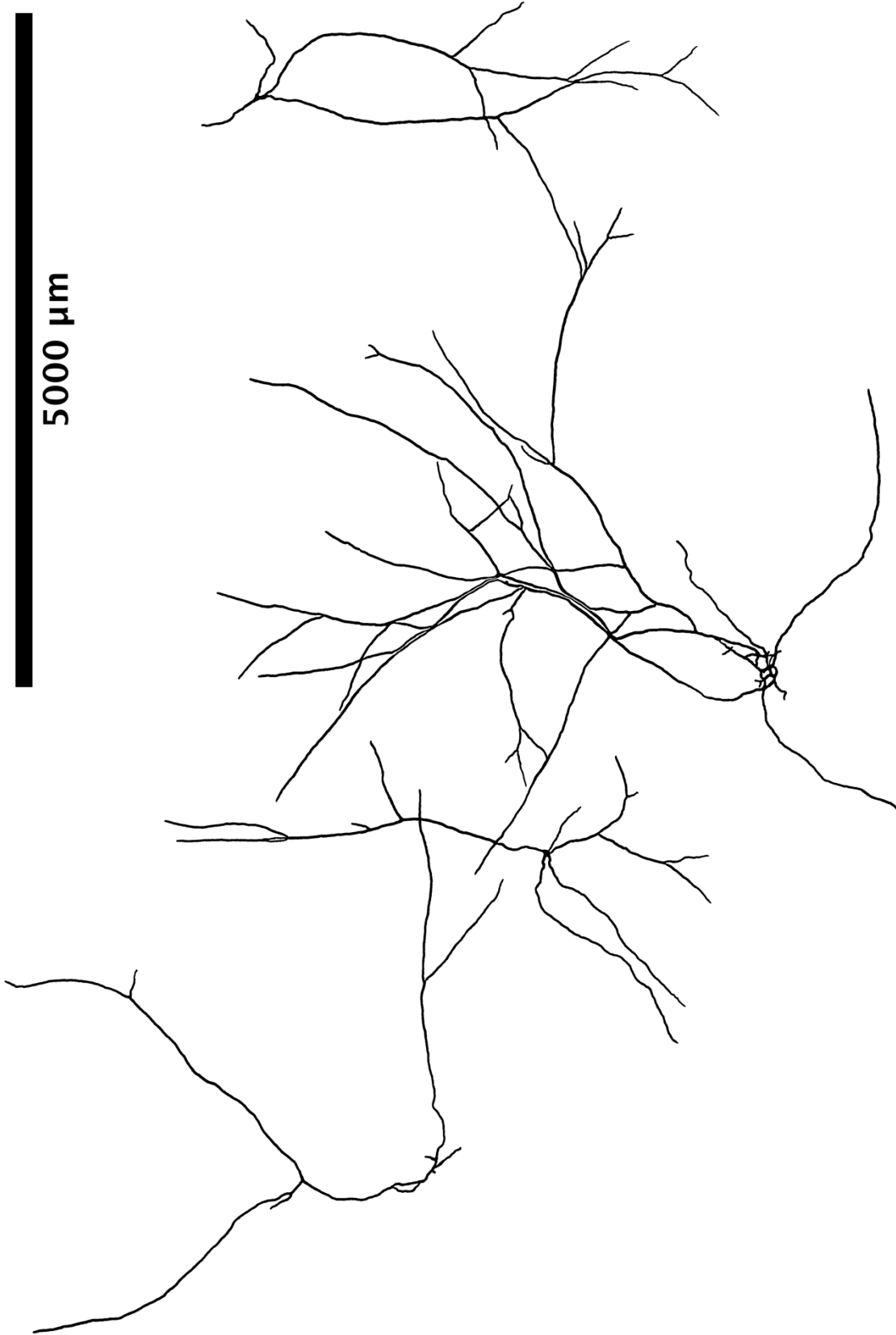


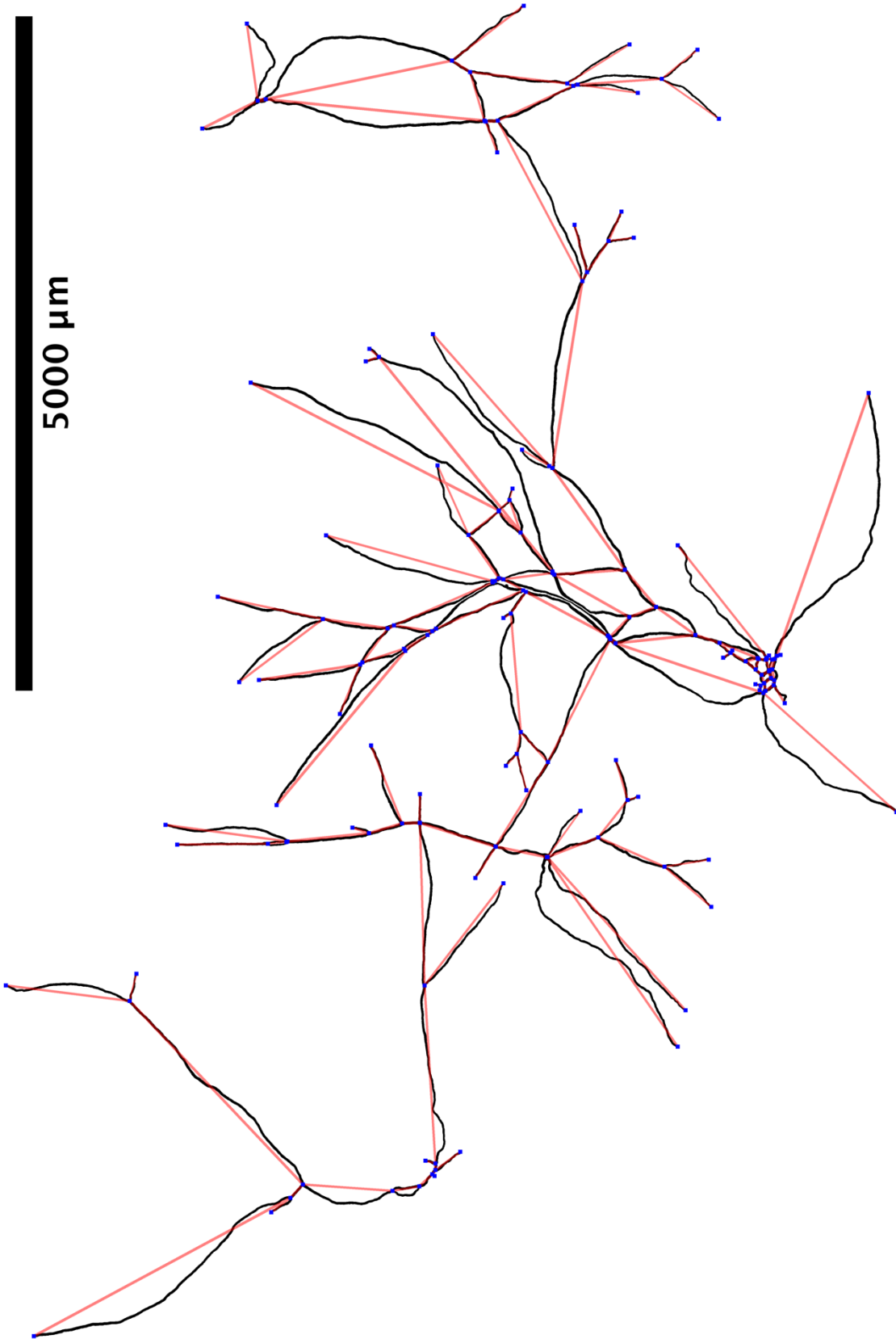


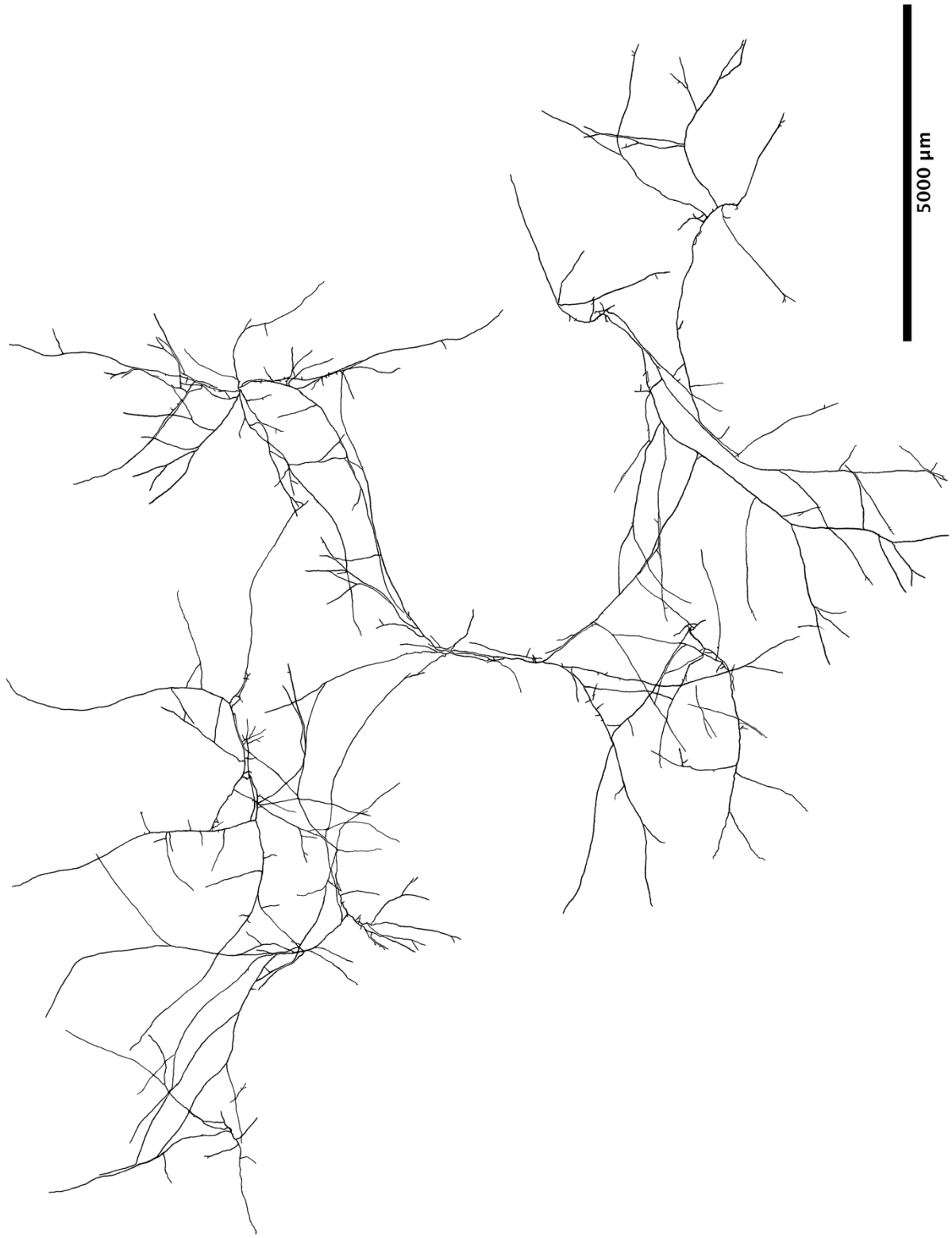
5000 μm

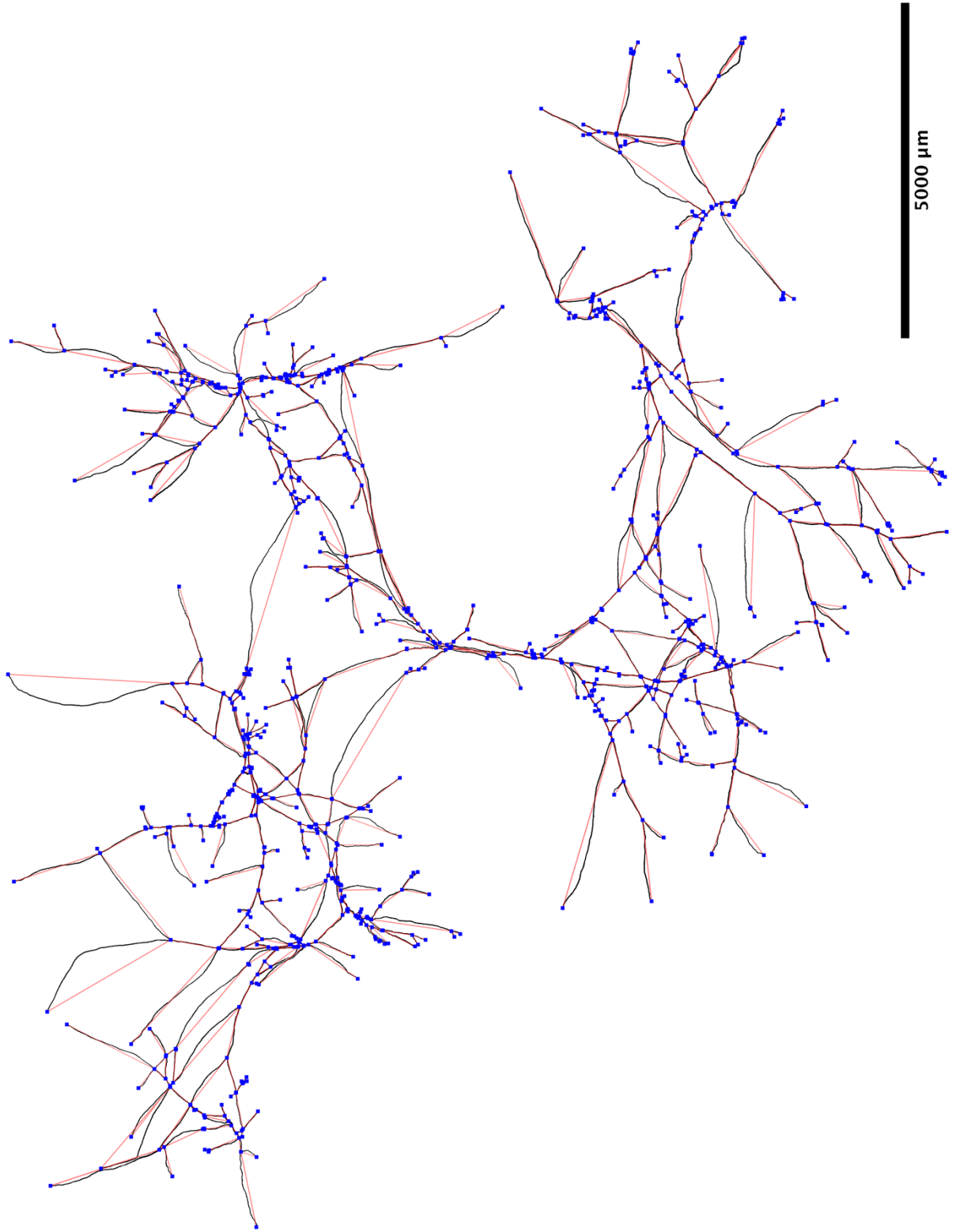












IV. Bibliography

- Akashi, T., Kanbe, T., & Tanaka, K. (1994). The role of the cytoskeleton in the polarized growth of the germ tube in *Candida albicans*. *Microbiology*, *140*(September), 271–280.
- Albert, R., & Barabási, A. L. (2002). Statistical mechanics of complex networks. *Reviews of Modern Physics*, *74*(1), 47–97.
<https://doi.org/10.1103/RevModPhys.74.47>
- Amaral, L. A. N., & Ottino, J. M. (2004). Complex networks. *The European Physical Journal B - Condensed Matter*, *38*(2), 147–162.
<https://doi.org/10.1140/epjb/e2004-00110-5>
- Ash, J. A., & Rapp, P. R. (2014). A quantitative neural network approach to understanding aging phenotypes. *Ageing Research Reviews*, *15*(1), 44–50.
<https://doi.org/10.1016/j.arr.2014.02.001>
- Baronchelli, A., Ferrer-i-Cancho, R., Pastor-Satorras, R., Chater, N., & Christiansen, M. H. (2013). Networks in Cognitive Science. *Trends in Cognitive Sciences*, *17*(7), 348–360. <https://doi.org/10.1016/j.tics.2013.04.010>
- Bebber, D. P., Hynes, J., Darrah, P. R., Boddy, L., & Fricker, M. D. (2007). Biological solutions to transport network design. *Proceedings of the Royal*

Society B: Biological Sciences, 274(1623), 2307–2315.

<https://doi.org/10.1098/rspb.2007.0459>

Blackwell, M., Hibbett, D. S., Taylor, J. W., & Spatafora, J. W. (2007). Research Coordination Networks : a phylogeny for kingdom Fungi (Deep Hypha). *The Mycological Society of America*, 98(April), 829–837.

Boccaletti, S., Latora, V., Moreno, Y., Chavez, M., & Hwang, D. U. (2006). Complex networks: Structure and dynamics. *Physics Reports*, 424(4–5), 175–308. <https://doi.org/10.1016/j.physrep.2005.10.009>

Boddy, L. (1999). Mycological Society of America Saprotrophic cord-forming fungi : meeting the challenge of heterogeneous environments. *Mycologia*, 91(1), 13–32.

Booking, S. P., Wiebe, M. G., Robson, G. D., Hansen, K., Christiansen, L. H., & Trinci, A. P. J. (1999). Effect of branch frequency in *Aspergillus oryzae* on protein secretion and culture viscosity. *Biotechnology and Bioengineering*, 65(6), 638–648. [https://doi.org/10.1002/\(SICI\)1097-0290\(19991220\)65:6<638::AID-BIT4>3.0.CO;2-K](https://doi.org/10.1002/(SICI)1097-0290(19991220)65:6<638::AID-BIT4>3.0.CO;2-K)

Boswell, G. P., & Hopkins, S. (2008). Linking hyphal growth to colony dynamics: Spatially explicit models of mycelia. *Fungal Ecology*, 1(4), 143–154. <https://doi.org/10.1016/j.funeco.2008.10.003>

Cairney, J. W. G. (2005). Basidiomycete mycelia in forest soils : dimensions , dynamics and roles in nutrient distribution. *The British Mycological Society*, 109(January), 7–20. <https://doi.org/10.1017/S0953756204001753>

Dikec, J., Olivier, A., Bobée, C., D'Angelo, Y., Catellier, R., David, P., Filaine, F., Herbert, S., Lalanne, C., Lalucque, H., Monasse, L., Rieu, M., Ruprich-Robert, G., Véber, A., Chapeland-Leclerc, F., & Herbert, E. (2020). Hyphal network whole field imaging allows for accurate estimation of anastomosis rates and branching dynamics of the filamentous fungus *Podospora anserina*. *Scientific Reports*, 10(1), 3131. <https://doi.org/10.1038/s41598-020-57808-y>

- Dirnberger, M., Kehl, T., & Neumann, A. (2015). NEFI: Network Extraction from Images. *Scientific Reports*, 5, 1–10. <https://doi.org/10.1038/srep15669>
- Druzhinina, I. S., Chenthamara, K., Zhang, J., Atanasova, L., Yang, D., Miao, Y., Rahimi, M. J., Grujic, M., Cai, F., Pourmehdi, S., Salim, K. A., Pretzer, C., Kopchinskiy, A. G., Henrissat, B., Kuo, A., Hundley, H., Wang, M., Aerts, A., Salamov, A., ... Kubicek, C. P. (2018). *Massive lateral transfer of genes encoding plant cell wall-degrading enzymes to the mycoparasitic fungus Trichoderma from its plant-associated hosts.*
- Finn, R. K. (1959). Theory of Agar Diffusion Methods for Bioassay. *School of Chemical and Metallurgical Engineering*, 31(6), 975–977.
- Harris, S. D., & Momany, M. (2004). Polarity in filamentous fungi : moving beyond the yeast paradigm. *Fungal Genetics and Biology*, 41(November), 391–400. <https://doi.org/10.1016/j.fgb.2003.11.007>
- Heath, I. B. (1990). The Roles of Actin in Tip Growth of Fungi. *International Review of Cytology*, 123, 95–127.
- Heaton, L., Obara, B., Grau, V., Jones, N., Nakagaki, T., Boddy, L., & Fricker, M. D. (2012). Analysis of fungal networks. *Fungal Biology Reviews*, 26(1), 12–29. <https://doi.org/10.1016/j.fbr.2012.02.001>
- Horio, T. (2007). Role of microtubules in tip growth of fungi. *J Plant Res*, 120(October), 53–60. <https://doi.org/10.1007/s10265-006-0043-2>
- Lecault, V., Patel, N., & Thibault, J. (2007). Morphological characterization and viability assessment of *Trichoderma reesei* by image analysis. *Biotechnology Progress*, 23(3), 734–740. <https://doi.org/10.1021/bp0602956>
- Lejeune, R., & Baron, G. V. (1997). Simulation of growth of a filamentous fungus in 3 dimensions. *Biotechnology and Bioengineering*, 53(2), 139–150. [https://doi.org/10.1002/\(SICI\)1097-0290\(19970120\)53:2<139::AID-BIT3>3.0.CO;2-P](https://doi.org/10.1002/(SICI)1097-0290(19970120)53:2<139::AID-BIT3>3.0.CO;2-P)
- Ma, Lopez-franco, R., & Bracker, C. E. (1996). Diversity and dynamics of the

- Spitzenkörper in growing hyphal tips of higher fungi. *Protoplasma*, 195(April), 90–111.
- Mendoza-mendoza, A., Clouston, A., Li, J., Nieto-jacobo, M. F., Cummings, N., Steyaert, J., & Hill, R. (2016). Chapter 2 Isolation and Mass Production of Trichoderma. *Methods in Molecular Biology*, 1477, 13–20.
<https://doi.org/10.1007/978-1-4939-6367-6>
- Mineyuki, Y. (2007). Plant microtubule studies : past and present. *J Plant Res*, 45–51. <https://doi.org/10.1007/s10265-006-0063-y>
- Newman, M. (2013). *Networks: An Introduction*. 15(1), 583–605.
<https://doi.org/10.1093/acprof>
- Newman, M. E. J. (2003). The structure and function of complex networks. *SIAM Review*, 45(2), 167–256. <https://doi.org/10.1137/S003614450342480>
- Pinto, C. A., Moreira, S. A., Fidalgo, L. G., Inácio, R. S., Barba, F. J., & Saraiva, J. A. (2020). Effects of high-pressure processing on fungi spores: Factors affecting spore germination and inactivation and impact on ultrastructure. *Comprehensive Reviews in Food Science and Food Safety*, 19(2), 553–573.
<https://doi.org/10.1111/1541-4337.12534>
- Reynaga-pen, C. G. (1997). Apical Branching in a Temperature Sensitive Mutant of *Aspergillus niger* 1. *Fungal Biology Reviews*, 167(June), 153–167.
- Reynaga-Peña, C. G., & Bartnicki-García, S. (2005). Cytoplasmic contractions in growing fungal hyphae and their morphogenetic consequences. *Archives of Microbiology*, 183(4), 292–300. <https://doi.org/10.1007/s00203-005-0771-z>
- Roca, M. G., Arlt, J., Jeffree, C. E., & Read, N. D. (2005). Cell Biology of Conidial Anastomosis Tubes in *Neurospora crassa*. *American Society for Microbiology*, 4(5), 911–919. <https://doi.org/10.1128/EC.4.5.911>
- Roncal, T., & Ugalde, U. (2003). Conidiation induction in *Penicillium*. *Research in Microbiology*, 154(8), 539–546. [https://doi.org/10.1016/S0923-2508\(03\)00168-2](https://doi.org/10.1016/S0923-2508(03)00168-2)

- Smith, M. L., Bruhn, J. N., & Anderson, J. B. (1992). The fungus *Armillaria bulbosa* is among the largest and oldest living organisms. *Nature*, *365*(April), 428–431.
- Steyaert, J. M., Weld, R. J., Mendoza-Mendoza, A., & Stewart, A. (2010). Reproduction without sex: Conidiation in the filamentous fungus *Trichoderma*. *Microbiology*, *156*(10), 2887–2900. <https://doi.org/10.1099/mic.0.041715-0>
- Trinci, A. P. J. (1973). The hyphal growth unit of wild type and spreading colonial mutants of *Neurospora crassa*. *Archiv Für Mikrobiologie*, *91*(2), 127–136. <https://doi.org/10.1007/BF00424756>
- Watts, D. J., & Strogratz, S. H. (1998). Collective dynamics of “small-world” networks. *Nature*, *393*(2), 440–442. <https://doi.org/10.1111/cobi.13031>
- Withers, J. M., Wiebe, M. G., Robson, G. D., & Trinci, A. P. J. (1994). Development of morphological heterogeneity in glucose-limited chemostat cultures of *Aspergillus oryzae*. *Mycological Research*, *98*(1), 95–100. [https://doi.org/10.1016/S0953-7562\(09\)80345-6](https://doi.org/10.1016/S0953-7562(09)80345-6)

Books:

- Jennings, D., H & Rayner, A. D. M., 1984, *The Ecology and Physiology of the Fungal Mycelium*, United Kingdom, Cambridge Univ. Press, Cambridge.
- Jímenez, L., Felipe, Merchant, Horacio, 2003, *Biología Celular y Molecular*, México, Pearson Educación, ISBN: 970-26-0387-0.
- Webster, J., & Weber, R. W., 2007, *Introduction to Fungi*, United Kingdom, Cambridge University Press, ISBN: 978-0-511-27783-2.

Official Standard:

- NOM-111-SSA1-1994. Norma Oficial Mexicana NOM-111-SSA1-1994, Bienes y servicios. Método para la cuenta de mohos y levaduras en alimentos.